

# Biomedical Applications of Multiferroic Nanoparticles

Armin Kargol<sup>1</sup>, Leszek Malkinski<sup>2</sup> and Gabriel Caruntu<sup>2</sup>

<sup>1</sup>*Department of Physics, Loyola University, New Orleans, LA*

<sup>2</sup>*Advanced Materials Research Institute, University of New Orleans, New Orleans LA  
USA*

## 1. Introduction

Magnetic nanoparticles with functionalized surfaces have recently found numerous applications in biology, medicine and biotechnology [1,2]. Some application concern in vitro applications such as magnetic tweezers and magnetic separation of proteins and DNA molecules. Therapeutic applications include hyperthermia [3], targeted delivery of drugs and radioactive isotopes for chemotherapy and radiotherapy and contrast enhancement in magnetic resonance imaging. In this chapter we describe an entirely new concept of using magnetic/piezoelectric composite nanoparticles for stimulation of vital functions of living cells.

The problem of controlling the function of biological macromolecules has become one of the focus areas in biology and biophysics, from basic science, biomedical, and biotechnology points of view. New approaches to stimulate cell functions propose using heat generated by hysteresis losses in magnetic nanoparticles placed in high frequency magnetic field (or magnetic nanoparticle hyperthermia) [5] and mechanical agitation of the magnetic nanoparticles which are attached to the cells using external low frequency magnetic field. In this chapter we propose a new mechanism to be explored which relies on localized (nanoscale) electric fields produced in the vicinity of the cells. Research in this field provides new insight into complexity, efficiency and regulation of biomolecular processes and their effect on physiological cellular functions. It is hoped that as our understanding of complex molecular interactions improves it will lead to new and important scientific and technological developments.

### **Magnetolectric properties of nanoparticles**

A magnetolectric is a generic name for the material which exhibits significant mutual coupling between its magnetic and electronic properties. Especially important group in this category are multiferroics which simultaneously demonstrate ferroelectricity and ferromagnetism. Although there exist a few examples of single phase multiferroics [6-11], the multiferric composites [7] with superior magnetolectric parameters are much more attractive for applications. These composites consist of mechanically coupled ferroelectric and ferromagnetic phases. The conversion of magnetic to electric energy takes advantage of piezoelectric (or more general electrostrictive) properties of the ferroelectric phase and piezomagnetic (or magnetostrictive) properties of the ferromagnetic phase. Magnetostrictive

stresses generated in the magnetic phase by the variation of the applied magnetic field  $\Delta H$  are transferred through the interface between the ferroic phases to the ferroelectric which in turn changes polarization  $\Delta P$  and associated electric field  $\Delta E$  due to the piezoelectric effect. Magnetoelectric coefficient  $\alpha$  is considered to be the figure of merit which characterizes the performance of a multiferroic composites. In the simplest case, the coefficient  $\alpha$  is defined as the ratio of the polarization change in response to the change of the field:  $\alpha = \Delta P / \Delta H$ . Alternatively, magnetoelectric voltage coefficient  $\alpha_E = \Delta E / \Delta H$  can be used instead.

In general, the response of the electric flux density  $\mathbf{D}$  in the multiferroic composites to the applied electric field  $\mathbf{E}$ , external stress  $\mathbf{S}$  and the magnetic field  $\mathbf{H}$  vectors is determined by the permittivity tensor  $\epsilon_{ij}$ , piezoelectric coefficients  $e_{ij}$  and the magnetoelectric coefficient tensor  $\alpha_{ij}$ :

$$D_i = \sum_{j=1}^{j=3} \epsilon_{ij} E_j + \sum_{j=1}^{j=6} e_{ij} S_j + \sum_{j=1}^{j=3} \alpha_{ij} H_j$$

The components of the magnetoelectric coefficient tensor depend on the piezoelectric coefficients of the ferroelectric, the piezomagnetic coefficients of the magnetic phase, geometry of the constituting components and the quality of the mechanical contact between the piezoelectric and magnetic phases. Examples of formulas for the magnetoelectric coefficients for laminated and particulate composites can be found in review papers by Nan et al. [7] and Bichurin et al. [12,13]. Vast majority of publications on multiferroic composites concerns particulate and laminar composites because of potential applications of these structures in magnetic-field sensors, magnetic-field-tunable microwave and millimeter wave devices, and miniature antennas, data storage and processing, devices for modulation of amplitudes, polarizations and phases of optical waves, optical diodes, spin-wave generation, amplification and frequency conversion.

So far, relatively little attention has been drawn to fabrication and characterization of composite nanoparticles. The multiferroic nanoparticles, which are useful for the particular application we propose, can be in the form of a spherical core-shell nanoparticles with a ferromagnetic core and a ferroelectric shell as depicted in Fig. 1 a), magnetic rods with a piezoelectric coating, as seen in Fig. 1b) (also concentric magnetic/piezoelectric tubes) as well as composite spheres of piezoelectric ceramics or piezopolymers with embedded magnetic nanoparticles (Fig.1c).

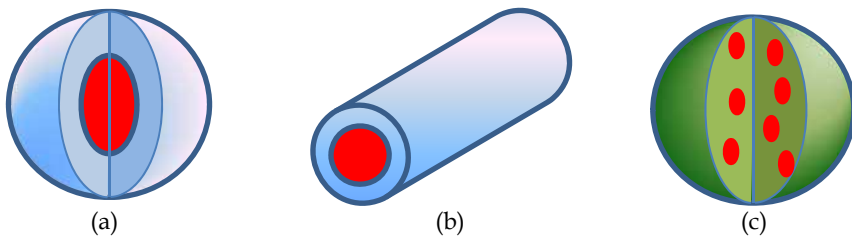


Fig. 1. Three types of the magnetoelectric nanoparticles: spherical core-shell nanoparticles with magnetostrictive core encapsulated in piezoelectric shell (a), cylindrical core-shell nanoparticle with magnetostrictive rod and piezoelectric coating (b) and a composite superparticle with magnetic nanoparticles embedded into piezo-polymer or piezo-ceramics (c).

The reasons for which these magnetoelectric particles are expected to have excellent magnetoelectric performance are as follows:

- a. Very good mechanical contact at the interface between two synthesized ferroic phases (which is an issue for many particulate or laminar composites bonded by gluing, pressing or sintering).
- b. Efficient transfer of magnetostrictive stresses to the piezoelectric phase. Because of very small thickness of the piezoelectric shell the magnetostrictive stress will be absorbed by the whole volume of the piezoelectric phase (not just by interfacial layer as it may happen in thicker film coatings or large grains). Here, it is important to mention that in our preliminary studies we did not observe any dramatic deterioration of piezoelectric or magnetostrictive properties of the constituting components of the nanoparticles as their dimensions decreased down to 25 nm.
- c. No substrate clamping effect which restricts magnetostrictive or electrostrictive strains in some laminated or thin film structures.

Since a few existing articles about magnetoelectric core-shell nanoparticles [12-20] do not report on their magnetoelectric coefficients our estimate of the expected properties of multiferroic nanoparticles will be based on the coefficients of the laminated composites. At this point it is important to note, that the record values of magnetoelectric voltage coefficient exceeding 90 V/(cm Oe) [7,21] have been measured for the laminated composites in magnetoacoustic resonance conditions.

Theoretical model by Petrov et al. [22] predicts even higher values (up to 600 V/cm Oe) of the  $\alpha_E$  at electromechanical resonance for the free standing multiferroic nanopillar structures, which can be identified with our cylindrical core-shell nanoparticles. However, because of specific frequency range (0-5000 Hz) which corresponds to ion channel dynamics we expect in our application the values of magnetoelectric voltage coefficient  $\alpha_E$  of the core-shell nanoparticles to be closer to the non-resonant values ranging from 1 to 5 V/ (cm Oe).

The difference of potentials generated by the particle will depend on the particle size. It is easy to estimate that nanoparticles as small as 50 nm with magnetoelectric voltage coefficient of 5V/(cm Oe) should be capable of generating voltage of 25 mV when exposed to the field of 100 Oe ( or 0.01 T). This voltage is sufficient to control ion transport through ion channels and also to trigger action potential in nerves. By increasing the size of the particles to 1 micrometer (which is still a small fraction of the cell size) this voltage can be increased by more than 2 orders of magnitude.

Whereas the magnetoelectric performance of the multiferroic core-shell nanoparticles can be elucidated to a high degree, there is not enough literature data available for the piezopolymer based composite nanoparticle. However, these nanoparticles are intriguing for at least three reasons:

- These composites may use superparamagnetic nanoparticles embedded in the piezopolymer. In the absence of the external field they will not display effective magnetic moment which prevents potential problems with particle aggregation.
- The key difference between the multiferroics and these piezopolymer clusters is that they may use different mechanisms for generation of electric fields. Because of mechanically soft matrix, attractive dipole-dipole interactions between magnetic nano-inclusions in the presence of a magnetic field may be more effective than the

- magnetostrictive strains of individual magnetic particle. The strained piezopolymer will respond by changing its polarization. The primary factors which will affect the performance of these magnetoelectric nanocomposites will be: saturation magnetization of the nanoparticles, separation between the particles and the piezoelectric coefficients of the piezopolymer, which can be as good as those of piezoelectric solids [23]. Due to insufficient literature data, good performance of these novel structures can be predicted based on excellent performance of piezopolymers in laminated composites [24].
- Some polymer composites are biocompatible and have already been successfully used in cancer research. Therefore, this design of magnetoelectric nanoparticles may be the ultimate solution in therapeutic applications.

### Voltage-gated ion channels

One of the primary examples of research on interaction of electromagnetic fields with biological macromolecules is the study of ion channels. Ion channels are membrane proteins that form pores for controlled exchange of ions across cellular membranes [24]. Their two main characteristics are their selectivity, i.e. the type of ions they flux (e.g.  $K^+$ ,  $Na^+$ , or  $Ca^{++}$ ) and their gating, i.e. the process of opening and closing in response to the so-called gating variable. Probably the most common are the voltage-gated ion channels which gate in response to the transmembrane electric field. They are central to shaping the electrical properties of various types of cells and regulate a host of cellular processes, such as action potentials in neurons or muscle contraction, including the heart muscle. Ion channel defects have also been identified as causes of a number of human and animal diseases (such as cystic fibrosis, diabetes, cardiac arrhythmias, neurological disorders, hypertension etc.) [25]. As such, ion channels are primary targets for pharmacological agents for therapeutic purposes. Cellular responses to various chemical stimuli, such as drugs and toxins, can be analyzed in terms of their effect on ion channels. From a biophysical standpoint ion channels are the primary examples of voltage-sensitive biomolecules.

The main aims of ion channel studies are to understand the channel gating kinetics and how it is affected by various external factors as well as to develop methods of controlling the channel gating. It is believed that this will lead to knowledge of corresponding molecular mechanisms of gating and eventually to a full understanding of the physiological role of the channels. Gating of voltage-gated ion channels results from rearrangements of the tertiary structure of the channel proteins, i.e. transitions between certain meta-stable conformational states in response to changes in transmembrane potential. Various conformations can be described by a finite set of states (closed, inactivated or open), connected by thermally activated transitions, and known as the Markov model of channel kinetics [26,27]. It can be mathematically described as a discrete Markov chain with transitions between the states given as:

$$\alpha(V) = \alpha(0)\exp(qV / kT) \quad (1)$$

where  $\alpha$  is a generic transition rate,  $V$  - membrane voltage,  $k$  - Boltzmann constant,  $T$  - temperature,  $q$  - gating charge. The topology of Markov models (i.e. the number and connectivity of its discrete states) as well as the parameters for the transition rates are determined by fitting model responses to various sets of experimental data, mostly obtained from electrophysiological experiments. It needs to be understood, though, that Markov models are only a coarse approximation and more precisely the channel gating should be viewed as a motion of a "gating particle" in a certain energy landscape, subject to thermal

fluctuations and governed by the Langevin or Fokker-Planck equation [28]. Models based on the Smoluchowski equation describing channel gating as a diffusion process in a one-dimensional energy landscape have also been developed [29-31]. However, a picture of channel gating as a discrete Markov chain with the discrete states corresponding to the minima in this energy landscape has been widely and very successfully used. A large proportion of scientific publications on ion channels is devoted to channel gating properties and the corresponding Markov models.

A functional model of a voltage-gated ion channel consists of three parts: the voltage sensor, the pore, and the gate. Commonly, the channels are made of four subunits ( $K^+$  channels) or one protein with four homologous domains ( $Na^+$  and  $Ca^{2+}$  channels). Each of these has six transmembrane segments S1-S6. It is believed that the voltage sensitivity of ion channel is based on the movement of the charged S4 domain (described as the movement of the "gating charge") that causes conformational changes of the molecule resulting in channel opening or closing [24].

### Ion channel electrophysiology

The bulk of experimental data on ion channel function comes from patch-clamping technique [24,32] (Fig. 2), in which the voltage across a cell membrane is controlled by a feedback circuit that balances, and therefore measures, the net current. Variations of this technique include whole-cell recordings (measured from a large number of ion channels), single channel recordings (ionic currents through membrane patches containing only single channels), and gating currents. Electrophysiological experiments have been recently complemented by X-ray crystallographic methods, fluorescence methods (FRET), and other imaging techniques [33-35].

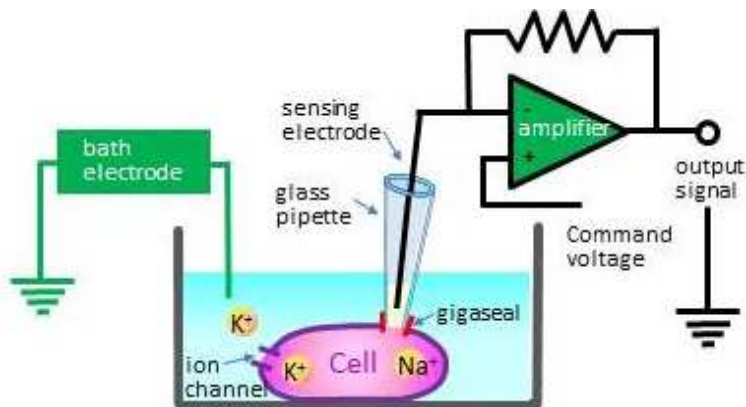


Fig. 2. A schematic illustration of the patch-clamp method

For electrophysiological experiments the channels can be either in their native cells or expressed in a suitable expression system (typically mammalian cells transfected with the channel DNA or *Xenopus laevis* oocytes injected with the RNA). A cell is placed in a grounded solution in a recording chamber under an inverted microscope. A glass pipette with another electrode is moved using a micromanipulator until it forms a tight seal (a gigaseal) with the

cell membrane. A patch-clamp amplifier overrides the membrane potential that naturally exists across a membrane in every living cell, and measures the current flowing through the ion channels. The current reflects the kinetics of channel gating. In the whole-cell mode it is the total current from all channels present in the cell, while in the single-channel mode it is recorded from one or few channels in the excised membrane patch.

The paradigm of ion channel electrophysiology is a stepwise change of the potential from the holding hyperpolarized value. Membrane depolarization changes the transition rates, according to (1), and affects the stationary probability distribution among all Markov states. The transitions are thermally activated and are stochastic in nature. The time constant of channel relaxation to a new probability distribution depends on voltage and the temperature, but it typically is of the order of few ms. Experiments with time-variable, including rapidly fluctuating voltages have been also proposed for various purposes [36-40] and they only require sufficient bandwidth of the recording apparatus, faster than the time scale of channel gating kinetics. Bandwidth in excess of 5 kHz can be easily obtained with standard equipment. Based on these and other types of experimental data Markov models have been developed for many known channels and can be found in literature [36,37].

Ion channels in cell membranes can be found in any of their conformational states with certain probabilities and can “jump” from one state to another in a random fashion. This probability distribution among these different states is determined by the channel kinetics and in equilibrium states cannot be directly controlled. In other words, the molecules cannot be “forced” into any particular state. However, the transition rates between different states in a Markov model are voltage-dependent and as the voltage is varied the probability distribution for channel conformational states changes. One should distinguish here between equilibrium and non-equilibrium distributions. The former are achieved in response to static voltages while the latter are achieved for fluctuating voltage stimuli. The idea of remote channel control is to enhance a probability of finding channel molecules in a selected state (open, closed, or inactivated) by driving them into a non-equilibrium distribution with fluctuating electric fields [38,39] (Fig. 2). This is an idea that might be new to biologists but has been well-researched in statistical physics, both theoretically and experimentally [41-45].

### **Control of channel gating using multiferroic nanoparticles**

While a significant progress has been made on the channel gating kinetics modeling, there hasn't been as much success in controlling the channel function. The primary approach has been the use of pharmacological agents that modify the gating kinetics or block the channel transiently or permanently [46]. This has been used both for research and therapeutic purposes. Ion channel function can be modified by many natural agents extracted from plants and animals as well as drugs developed for that specific purpose. This has been the basis for treatment for many ion channel-related disorders. On the other hand ion channels are very difficult targets for pharmacological agents since their function is state and voltage dependent and the interactions are highly nonlinear. In this chapter we discuss a different, innovative approach, based on using multiferroic nanoparticles introduced extra- or intracellularly to locally modify electric fields and invoke appropriate conformational changes of channel proteins. This method would allow remote control of ion channel gating by externally applied magnetic fields.

Electric and magnetic fields have been shown to influence biological systems. The effect depends on the intensity and frequency of the fields and may be beneficial, adverse, or neutral to the organism. Only relatively gross effects, such as cell damage by electroporation or tissue heating by microwaves, are reasonably well understood [47-52]. Otherwise little is known about the mechanism of the interaction, and even the significance of the effect can be questioned. Some issues, like the adverse effects of electromagnetic fields generated in the vicinity of power lines or of microwave radiation from cell phone use are quite controversial [47,49,52]. On the other hand there are therapeutic uses of electric and/or magnetic fields. For instance, electro-stimulation techniques such as transcutaneous electrical nerve stimulation (TENS) or deep brain stimulation (DBS) have evolved from highly experimental to well-established therapy used for treatment of pain, epilepsy, movement disorders, muscle stimulation, etc. [53,54]. Although they provide evidence for the interaction of electric fields with biological systems these methods have many restrictions and drawbacks. First of all, many of present electrostimulation methods use high voltage (sometimes above 200V) and expose large portions of tissues or whole organs to electric fields and currents. Moreover, some internal organs (e.g. brain) are not accessible to electrostimulation without surgery. Secondly, the best results in therapy and research have been achieved using percutaneous electrodes which are in direct contact with bodily fluids.

The new method we propose is based on remote generation of local electric fields in the proximity of the cells by nanoparticles of magnetoelectric composites. Therefore, individual cells or selected groups of cells can be targeted, rather than whole tissues, and the voltage required for their stimulation will be of the order of several mV, not hundreds of volts. Also, because of the remote way in which the stimulation will be performed, the functions of the cells in the internal organs, including brain, can be controlled. Moreover, because of the magnetic component the particles can be concentrated in a specific location (of the brain, for instance) using magnetic field gradient. Finally, the nano-electrostimulation can target specific types of cells or even certain parts of cell membranes. This selectivity of stimulation can be achieved by functionalizing the surface of the nanoparticles and binding them to cells through antigens.

Figure 3 illustrates the proposed method for controlling ion channel gating. Multiferroic nanoparticles will be either placed in extracellular medium or introduced internally. When an external magnetic field is applied these multiferroic particles will respond to it and convert it to localized electric fields. For particles placed near cell membranes containing ion channels this will lead to local membrane depolarization or hyperpolarization. The ion channels would respond by opening or closing accordingly. The stimulating magnetic field can be generated e.g. by Helmholtz coils and hence its properties can be very easily controlled. Moreover, the field can be applied globally (i.e. to the selected parts or to the entire organism) but the electric fields will be generated only locally, in the areas to which nanoparticles have been delivered. By modifying the properties of the stimulating magnetic field, such as its strength, duration, and spectral properties, as well as by controlling the delivery locations for the nanoparticles, we achieve a tight control over the localized electric fields. This will lead to very localized changes in ion channel gating. The resulting changes in ionic currents can be measured using standard electrophysiological techniques.

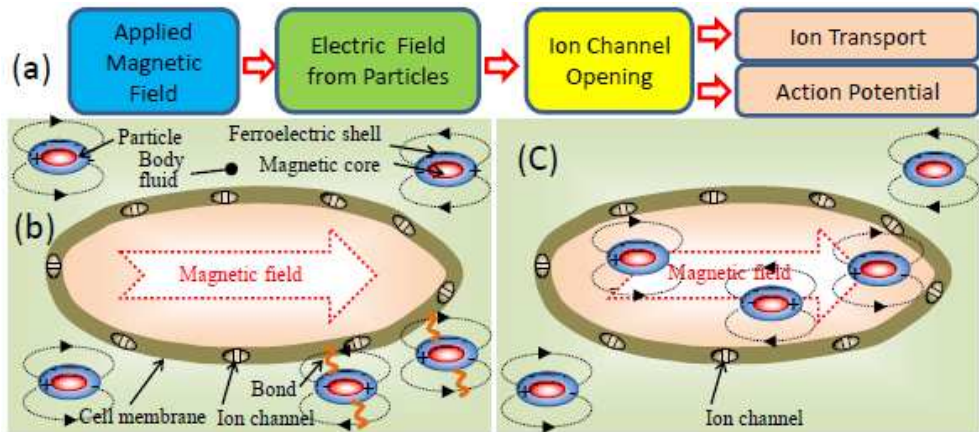


Fig. 3. Illustration of possible mechanisms of stimulation of ion channels by dipolar electric fields from magnetoelectric nanoparticles generated remotely by external magnetic field: (a) A chain of actions triggered by the applied magnetic field pulses. (b) External stimulation of the ion channels using nanoparticles in body fluid or particles bound to the cell membranes. (c) Internal stimulation of cells by uptaken nanoparticles.

The minimum strength of the signals used to control ion channels is of the order of mV and maximum frequency to which they respond should not exceed the typical bandwidth of the patch-clamping apparatus (few kHz). The purpose of the first experiments would be to determine the existence and the scale of this effect in mammalian cells *in vitro*, as well as its possible future biomedical applications.

Typical electrophysiology experiments include measurement of activation and “tail” ionic currents (Fig. 4). The former are recorded in response to stepwise voltage increases from the holding potential to a series of depolarizing values. The currents reflect the channels’ opening as a result of the depolarizing stimulus. The “tail” currents are recorded when the potential is changed from a depolarized value to a series of repolarizing values and show the process of channel closing in response to a hyperpolarizing stimulus. Similar types of recordings can be performed in the presence of nanoparticles and we can observe how the process of channel gating (opening or closing) is affected by the nanoscale electric fields generated by magnetically stimulated nanoparticles. It is expected that if a sufficient number of nanoparticles is placed close to the ion channels, there will be observable changes in the value and the time course of the ionic currents. The next step will be to apply modulated magnetic fields to generate variable electric fields that would allow us to directly impact the channel gating using remote stimulation. Both extracellular and intracellular application of nanoparticles can be tested.

It is important to mention that both the extracellular and intracellular action of the particles can be investigated (Fig. 5). Extracellular delivery is very straightforward. The nanoparticles will be dispersed in the extracellular medium. Since the ferroelectric component can be charged the multiferroic particles in the vicinity of the cells will be attracted to the cell membranes. For intracellular delivery, two methods can be contemplated. One is the particle uptake by cells that has been reported in several studies for particles of size up to 1.5  $\mu\text{m}$  [10].



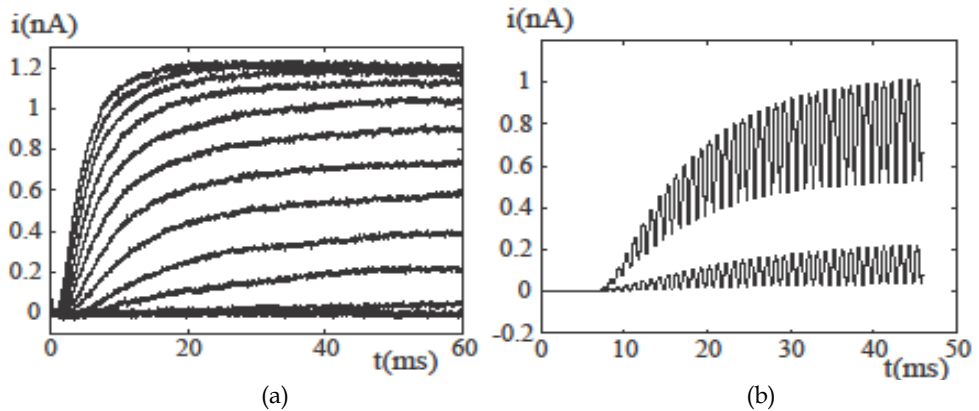


Fig. 4. Sample whole-cell currents recorded from Shaker K<sup>+</sup> channels using patch-clamp technique. a) Currents obtained for stationary voltages. At  $t = 0$  voltage was changed from a holding value of  $-70$  mV to a series of values varying from  $-70$  to  $42$  mV in  $8$  mV steps. b) Currents obtained for sinusoidally modulated voltages. The voltage amplitude was  $90$  mV peak-to-peak, the frequency  $1$  kHz, and the mean values:  $0$  mV and  $-30$  mV. It is expected that a similar modulation of current can be observed when ion channels are exposed to multiferroic nanoparticles and a modulated external magnetic field is applied.

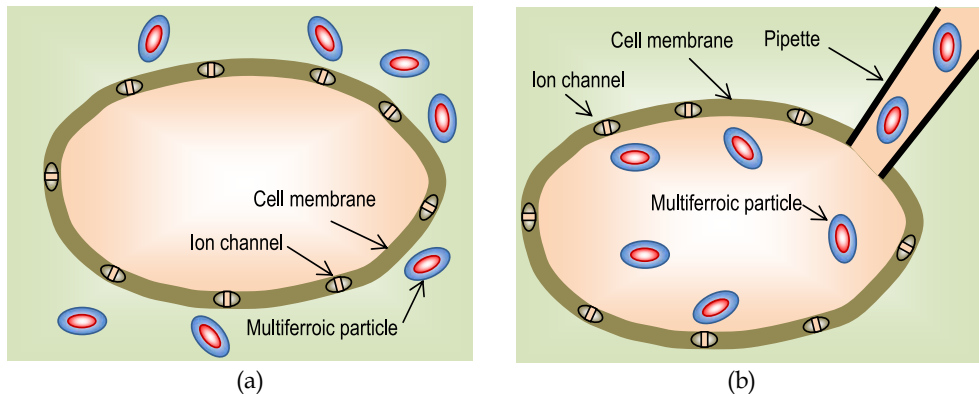


Fig. 5. Two possible methods for multiferroic nanoparticles: a) nanoparticles are dispersed in the extracellular medium.; b) patch-clamping pipette is filled with solution containing multiferroic nanoparticles. After the gigaseal is formed and the membrane patch at the tip of the pipette ruptured, the cell is perfused with the pipette solution, including the nanoparticles. The in-vivo uptake of nanoparticles into cells has been also reported after they are initially introduced extracellularly

Another method would make use of the recording apparatus used in patch-clamping. In the whole-cell mode the membrane patch at the tip of the recording pipette is ruptured, allowing a direct contact between the cell cytosol and the pipette solution. Since the volume of the pipette is significantly larger than the cell itself, the cell is quickly perfused with the pipette solution. If the nanoparticles are added to the pipette solution they quickly diffuse to

the cell interior. It is a method commonly used for intracellular drug delivery or recording solution replacement in ion channel research. For a precisely timed and controlled cell perfusion with different solutions an electronic valve controller can be used.

An ultimate goal would be using nanoparticles tethered to, or covered by ligands that bind to the selected membrane protein, in this case ion channel, ensuring that the nanoparticle stays in the vicinity of the target molecule. Fluorescent labels can be used in order to detect and track the multiferroic particles inside the cells.

It seems that there is no alternative to the magnetoelectric composites for generation of highly localized strong electric field in biological systems. At this point it is worth to mention that the pulses of magnetic flux ranging from  $10^3$  to  $10^6$  T/s used in the brain studies can induce only weak electromotive forces of the order of nanovolts to microvolts on cellular level and are more effective only on the scale of whole organs [2].

One can question the choice of multiferroic particles for generation of electric fields on sub-cellular level over the inductive systems which can also remotely generate local electric fields. A simple estimate shows that it would be extremely difficult to fabricate inductive systems with the micrometer size which would be capable of generating voltages sufficient to affect ion channels. Such circuits could be made by means of nanolithography (electron beam writing or focused ion beam etching) or by coating the nanostructures which have chiral shape (for example some ZnO nanowires or carbon nanotubes, which can grow in the chiral shape). According to the Faraday's law the voltage  $\varepsilon$  generated by a miniature coil is proportional to the number of turns  $n$  of the coil, its area  $S$  and the rate  $\partial B/\partial t$  of magnetic flux density  $B$  through the coil in the axial direction of the coil:

$$\varepsilon = -\frac{\partial\Phi}{\partial t} = -nS\frac{\partial B}{\partial t} \quad (2)$$

where  $\Phi$  is the magnetic flux. Microscopic coils with  $n=10$  turns and the size of  $1 \times 10^{-6}$  m (and the corresponding area  $S=10^{-12}$  m<sup>2</sup>) can be fabricated using current nanolithographic methods. When placed in the alternating magnetic field with the amplitude  $B=0.1$  Tesla and frequency of 1 kHz, such coils are expected to generate voltage of the order of  $10^{-9}$  V (or nanovolts rather than a fraction of volt) which is orders of magnitude smaller than that required for ion channel stimulation. This signal can be further enhanced by a factor of 1000 by inserting a magnetic core of magnetically soft material, but the signals generated by such inductors will still be below the useful range.

In contrast, multiferroic particles seem to be much more promising for generation of mV signals at micron- or nano-scale. As already mentioned, the strains of magnetostrictive material due to applied magnetic field produce deformation of the piezoelectric component which results in change of polarization of the particle. For the 1 micrometer magnetoelectric particles with medium magnetoelectric voltage coefficient of 1V/cmOe (measured in non-resonant conditions of 1 kHz) the same fields of 0.1 T can potentially generate voltage of 100 mV and even more than 10 times smaller particles can generate useful electric potentials for the stimulation of mammalian cells. The volume of these particles can be million times smaller than the size of a typical mammalian cell, thus they can easily be accommodated inside the cells. Also because of small size the nanoparticles can easily propagate with the bloodstream through the vascular system and with the static magnetic field they can be

directed to specific organs. Cells of these organs and ion channels closest to the multiferroic particles will experience presence of electric field when alternating magnetic field with the frequency in the acoustic range is applied. These local fields are expected to affect opening and closing of the ion channels and thus to alter ion transport across cell membranes.

### **Synthesis of core-shell magnetoelectric architectures**

#### *The role of the interfaces in the strain-mediated magneto-electric coupling*

A key requirement for achieving a sizeable ME response in composite materials is to combine phases with a robust piezomagnetic and piezoelectric properties. Perovskites  $ABO_3$  (A=alkaline/alkali earth metal, Pb; B=Ti, Zr, Nb, etc.) and ferrites (either spinel  $MFe_2O_4$  (M=transition metal) or M-type hexagonal ferrites  $AFe_{12}O_{19}$  (A=alkali earth metal) are good candidates for the design of ME nanocomposites since they present robust ferroelectric and magnetic responses at room temperature, are structurally compatible, have high chemical, thermal and mechanical stability, can be fabricated by simple methods at relatively low costs and present immiscibility gaps which limit the number of secondary phases. Recent advances in the chemical synthesis of nanoscale spinel-perovskites magnetoelectric structures resulted in materials that are approaching the quality needed for practical devices.

Since the control of the ferroic order parameters in magnetoelectric composites is dependent on how efficiently the generated strain is transferred across the shared interfaces, the intrinsic surface stress, the curvature of the surface [55], the contact area and the characteristics of the interfaces at the atomic scale are critical for the enhancement of the ME coupling. Any imperfect interface will more or less reduce the transfer of the elastic strain between the magnetostrictive and ferroelectric phases, thereby leading to a decrease of the ME response of the nanocomposites. The common methods of bonding two constituent phases in bulk magnetoelectrics include co-sintering [56,57], tape-casting [58], hot pressing [59] or adhesive bonding [60], which inevitably results in losses at the interface [61]. Furthermore, the elastic coupling between the constituent phases can be hindered by the formation of undesired phases as a result of the interdiffusion and/or chemical reactions during the annealing, thermal expansion mismatch between the two phases, as well as the presence of voids, residual grains, phase boundaries, porosity, dislocations and clamping effects [61,62].

Nanostructuring, as mentioned before, is an efficient way to engineer the interphase boundaries in hybrid ME composites which will lead to a maximum transfer of the mechanical strain between the two phases and, in turn will allow for an optimum conversion between the magnetic field and the electric field. Interfacing a ferroelectric with a ferromagnetic material in core-shell geometry offers a much higher anisotropy and high surface contact between the components which can also result in a strong ME effect. The low processing temperatures associated characteristic to the solution-mediated routes are preferable to substantially reduce the diffusion pathways between the molecular species, thereby preventing the formation of unwanted secondary phases. Magnetoelectric nanocomposites formed by assembling ferrites as the magnetic phase with perovskites as the electrostrictive phase can present a large ME response due to the large magnetostriction of the ferrites and the large piezoelectric coefficients of the perovskites. Additionally, in core-shell geometry the magnetic grains are completely isolated from each other by the

perovskite shells, which prevents the high dielectric losses related to electrical conduction, space-charge effects and Maxwell-Wagner interfacial polarization which are detrimental for the ME properties of the composites [64]. Last, but not least, the control of the size of the core and thickness of the shell enables the fine adjustment of the microstructure and phase fraction of the composites, resulting in materials with tunable properties and reproducible characteristics.

#### *Chemical synthesis of core-shell ME ceramic nanocomposites*

Soft chemistry-based chemical approaches represent a viable alternative to the classical “shake and bake” methods for the fabrication of metal oxide-based magnetoelectric nanocomposites. It is well known that the application of high temperatures in conventional sintering processes yields the formation of unwanted phases as a result of chemical reaction. For example undesired phases such as  $\text{BaFe}_{12}\text{O}_{19}$ ,  $\text{BaCo}_6\text{Ti}_6\text{O}_{19}$  or hexagonal  $\text{BaTiO}_3$  could appear in the  $\text{BaTiO}_3$ - $\text{CoFe}_2\text{O}_4$  ferroelectric magnetostrictive composites being very detrimental to their physical properties. In addition, the interphase diffusion of the constitutional atoms, though difficult to prove experimentally, lowers the local eutectic point around the boundary region, thereby facilitating the formation of structural defects in high concentration as well as liquid phases. These phenomena are detrimental to the piezoelectric signal and/or magnetostriction of the constituent phases and the strain created at the interface between them. Moreover, the large thermal expansion mismatch between the perovskite and ferrite phases deteriorates the densification and leads to the formation of micro-cracks. Solution-based methods alleviate these problems since they have the potential to achieve improved chemical homogeneity at molecular scale which significantly increases the surface contact between the two phases and, in turn, induces a notable enhancement of the magnetoelectric voltage coefficient.

Last, but not least, when ME nanocomposites are fabricated by chemical routes, diffusion distances are reduced on calcination compared to conventional preparation methods owing to the mixing of the components at colloidal or molecular level that favors lower crystallization temperatures for multicomponent oxide ceramics. This will eliminate the intermediate impurity phases leading to materials with small crystallites and a high surface area. Another challenges that need to be overcome are those related to the coupling between the two phases and include: a) the mechanical coupling between two phases must be in equilibrium; b) mechanical defects, such as the pores or cracks should be as low as possible to ensure a good mechanical coupling between the two phases; c) no chemical reaction between the constituent phases should occur during the synthesis; d) the resistivity of magnetostrictive phase should be as high as possible and the magnetic grains should be isolated from each other to minimize the leakage currents and prevent the composites from electric breakdown during electric poling; e) the magnetostriction coefficient of piezomagnetic phase and piezoelectric coefficient of piezoelectric phase must be high; and f) the proper poling strategy should be adopted to get high ME output in composites. Due to their assembled structure, core-shell piezoelectric-ferro/ferrimagnetic nanostructures have been fabricated exclusively by chemical routes. In the following we will briefly review the most relevant approaches described in the literature, as well as explore some novel methods which can be extended to the fabrication of ME core-shell ceramic nanoparticles with controlled morphology and predictable multiferroic properties.

### Synthesis of core-shell magnetoelectric ceramic nanocomposites and assemblies

The synthesis of core-shell spinel-perovskite nanoparticles (0-2 connectivity scheme) is conventionally carried out in two successive steps: (1) the precipitation of the ferrite nanoparticles and (2) the creation of a perovskite shell around each nanoparticle (Figure 6).

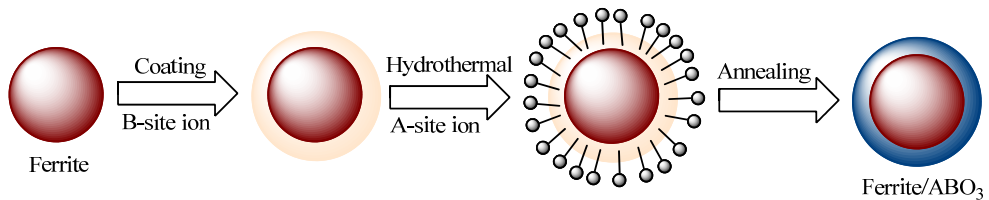


Fig. 6. Schematic of the two-step approaches used for the fabrication of core-shell ferrite/perovskite nanoparticles by soft-solution routes

Due to their low percolation threshold, the agglomeration of the ferrite nanoparticles should be avoided during the creation of the perovskite shells in order to prevent short-circuits during the measurement of their magnetoelectric properties. In general, the ferrite nanoparticles are obtained by classical alkaline precipitation of stoichiometric mixtures of  $\text{Fe}^{3+}$  and  $\text{M}^{2+}$  ( $\text{M}=\text{Mn, Fe, Co, Ni, Cu, Zn}$ ) in aqueous solutions. Liu and coworkers prepared spinel ferrite-perovskite core-shell nanoparticles by combining a solvothermal route with conventional annealing [65]. In the first step of the synthesis spheroidal iron oxide microparticles ( $\text{Fe}_3\text{O}_4$ ,  $\gamma\text{-Fe}_2\text{O}_3$  and  $\text{CoFe}_2\text{O}_4$ ) were obtained by treating hydrothermally solutions containing the metal ions and NaOH dissolved in ethylene glycol at 200 °C. The scanning electron microscopy (SEM) images shows that the as-prepared particles are spheroidal and have rough surfaces, are aggregate-free and have an average diameter of 280 nm. In the next step the ferrite nanoparticles were individually coated with a Ti hydroxide layer upon the slow hydrolysis and condensation during the aging of a solution of  $\text{Ti}(\text{SO}_4)_2$  in which the particles were suspended. The Ti hydroxide layers have a thickness of several tens on nanometers (Figure 7f) and they render the surface of each ferrite microparticles very smooth (third image in Figure 6 and Figures 7b and c). Furthermore, the hydroxide layer can be converted into a uniform and dense perovskite coating by *an in-situ* hydrothermal reaction at 140 °C between the  $\text{Pb}^{2+}$  ions from the solution and the  $\text{Ti}^{4+}$  ions anchored onto the surface of the magnetic particles. Because the perovskite layer has a low crystallinity, the resulting magneto-electric core-shell nanoparticles were subjected to an additional annealing in air at 600 °C.

X-Ray diffraction analysis confirmed that the nanocomposites are polycrystalline and free of secondary phase and consist of a spinel and perovskite phase suggesting that the proposed methodology can be used for the fabrication of core-shell nanoparticles with different chemical compositions (Figure 8a). Changing the chemical identity of the  $\text{M}^{2+}$  ions in the ferrite structure allows the tuning of the magnetic properties of the nanocomposites in a wide range. In general the coercivity of the nanocomposites increases upon annealing with  $H_c$  values of the nanocomposites of 15, 38, 40 and 1200 Oe for the  $\text{Fe}_3\text{O}_4/\text{PbTiO}_3$ ,  $\gamma\text{-Fe}_2\text{O}_3/\text{PbTiO}_3$ ,  $\gamma\text{-Fe}_2\text{O}_3/\text{Pb}(\text{Ti, Zr})\text{O}_3$  and  $\text{CoFe}_2\text{O}_4/\text{PbTiO}_3$  particles, respectively (Figures 8b and c).

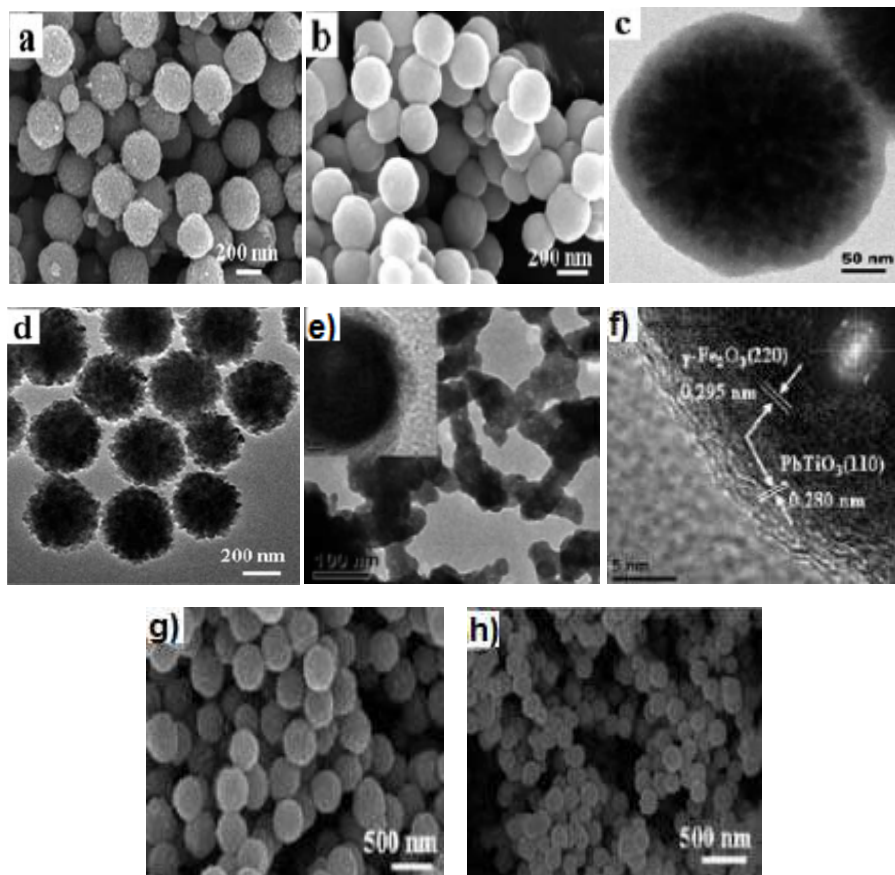


Fig. 7. SEM images of  $\text{Fe}_3\text{O}_4$  nanoparticles obtained under solvothermal conditions from polyol solution (a);  $\text{Fe}_3\text{O}_4$  microparticles coated individually with a layer of Ti hydroxide (b) and (c);  $\text{Fe}_3\text{O}_4/\text{PbTiO}_3$  core-shell particles (d); (e) and (f) TEM and HRTEM images of chain-like aggregates of  $\gamma\text{-Fe}_2\text{O}_3/\text{PbTiO}_3$  core-shell nanoparticles; SEM images of  $\text{CoFe}_2\text{O}_4/\text{BaTiO}_3$  (g) and  $\text{CoFe}_2\text{O}_4/\text{PbTiO}_3$  core-shell nanoparticles (h);

The values of the saturation magnetization were found to be in agreement with the molar fraction of the ferrite phase, as well as the average diameter of the magnetic core. These nanostructures are not dispersible in solvents, which somehow limits their use in biomedical applications. From the viewpoint of their magnetic and electric properties they were characterized in detail; however, no studies on their *magnetoelectric properties* were reported so far. A similar approach was proposed by Buscaglia and coworkers, who reported on the preparation of  $\alpha\text{-Fe}_2\text{O}_3@/\text{BaTiO}_3$  [65] and  $\text{Ni}_{0.5}\text{Zn}_{0.5}\text{Fe}_2\text{O}_4@/\text{BaTiO}_3$  [66] core-shell submicron particles. Similar to the method reported by Liu *et al.* ferrite nanoparticles were prepared by co-precipitation and then a uniform layer of amorphous titania ( $\text{TiO}_2$ ) was formed around each nanoparticle by treating a solution containing these magnetic grains with a peroxotitanium solution followed by a treatment of the nanoparticles with a solution of

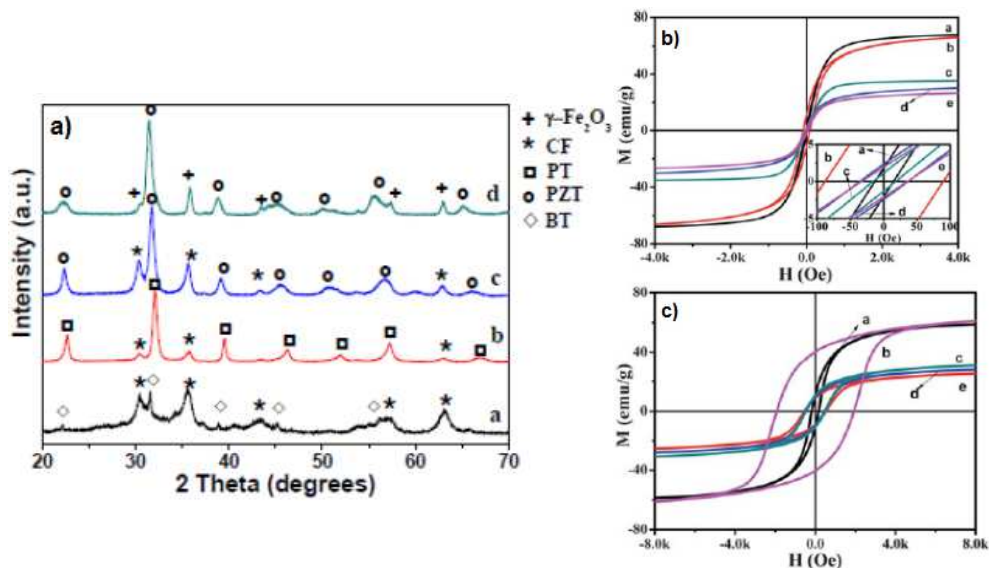


Fig. 8. XRD patterns of core-shell nanostructured powders of SEM images of  $\text{CoFe}_2\text{O}_4/\text{BaTiO}_3$  (a);  $\text{CoFe}_2\text{O}_4/\text{PbTiO}_3$ ;  $\text{Fe}_3\text{O}_4$  (b);  $\text{CoFe}_2\text{O}_4/\text{Pb(Ti, Zr)TiO}_3$  (c) and  $\gamma\text{-Fe}_2\text{O}_3/\text{PbTiO}_3$  (d) nanoparticles. Magnetic hysteresis loops of  $\text{Fe}_3\text{O}_4$  (a);  $\gamma\text{-Fe}_2\text{O}_3$  (b);  $\text{Fe}_3\text{O}_4/\text{PbTiO}_3$  (c);  $\gamma\text{-Fe}_2\text{O}_3/\text{PbTiO}_3$  (e);  $\gamma\text{-Fe}_2\text{O}_3/\text{Pb(Ti, Zr)O}_3$  nanoparticles (upper panel) and the as-prepared  $\text{CoFe}_2\text{O}_4$  nanoparticles (a) and after annealing at 600 °C (b) and  $\text{CoFe}_2\text{O}_4/\text{BaTiO}_3$  (c);  $\text{CoFe}_2\text{O}_4/\text{PbTiO}_3$  (d) and  $\text{CoFe}_2\text{O}_4/\text{Pb(Ti, Zr)O}_3$  (e) nanopowders, respectively

$\text{BaCO}_3$  nanoparticles. A heat treatment at 700 °C in air ensured the formation of the perovskite layer on the surface of the magnetic nanoparticles. From a mechanistic viewpoint, it is believed that  $\text{BaCO}_3$  selectively binds titania on the surface of the magnetic grains, thereby promoting the diffusion of the  $\text{Ba}^{2+}$  and  $\text{O}^{2-}$  ions from the  $\text{BaTiO}_3/\text{BaCO}_3$  interface to the  $\text{BaTiO}_3/\text{TiO}_2$  interface throughout the perovskite lattice with the preservation of the initial titanium-containing layer and preserving a good dispersion of the particles [67-69].

As seen in Figure 9a, the as-prepared  $\alpha\text{-Fe}_2\text{O}_3$  particles are spheroidal with narrow edges and an average diameter of 400-500 nm. These particles increase their sizes upon the coating with the perovskite layer (Figure 9d) yielding porous powders formed by 300-600 nm grains with a certain degree of inherent aggregation after the heat treatment (Figures 9b and c). Although this method allows the variation of the molar fraction of the nanostructured ferrites, as well as their chemical composition, the phase analysis revealed that the resulting two-phase composites are slightly contaminated with secondary phases, such as  $\text{BaFe}_{12}\text{O}_{19}$ , and  $\text{Ba}_{12}\text{Fe}_{28}\text{Ti}_{15}\text{O}_{84}$  which can be potentially detrimental to their magnetoelectric properties.,

HRTEM microscopy experiments revealed that the hexagonal ferrites form as secondary phases when the amount of  $\text{BaTiO}_3$  in the composite was decreased from 73% (wt.) to 53% (wt.), whereby the nanocomposites seem to be coated with a 20-30 nm thick  $\text{BaTiO}_3$  glassy layer separated by a thin (3-5 nm) interdiffusion region (Figure 9c). Such a behavior was ascribed to the formation of an eutectic during sintering, despite the fact that liquid phases were not found on the isothermal section ( $t=1200$  °C) of the phase diagram. The microstructural

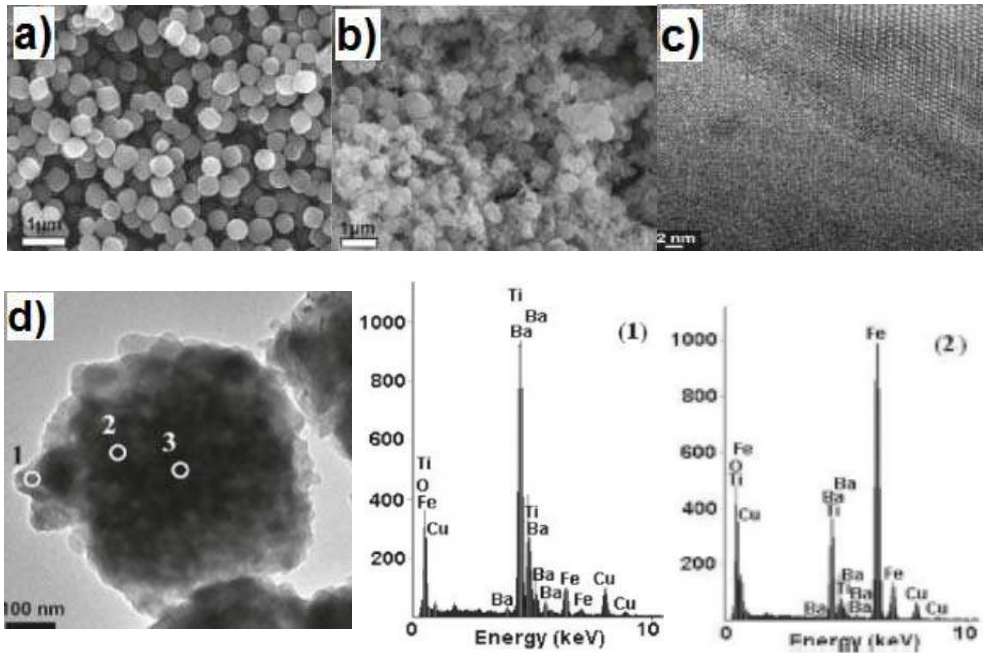


Fig. 9. SEM images of the  $\alpha$ -Fe<sub>2</sub>O<sub>3</sub> nanoparticles and  $\alpha$ -Fe<sub>2</sub>O<sub>3</sub>/BaTiO<sub>3</sub> composite particles with 73% (b) and 53% (wt.) (c) BaTiO<sub>3</sub> core-shell nanostructured powders after annealing at 1100 °C; (d); TEM image of a single  $\alpha$ -Fe<sub>2</sub>O<sub>3</sub>/BaTiO<sub>3</sub> composite particle with 73% BaTiO<sub>3</sub> and the corresponding EDX spectra for points 1 and 2 in Figure 4d;

study of the Ni<sub>0.5</sub>Zn<sub>0.5</sub>Fe<sub>2</sub>O<sub>4</sub>@BaTiO<sub>3</sub> core-shell particles revealed that they are constructed by quasi-spherical nickel ferrite particles with an average diameter of 600 nm onto which have been attached needle-like BaTiO<sub>3</sub> nanograins with a length of 130 nm and an average diameter of 57 nm. The dielectric constant has values which are lower than those of the pristine perovskite phase. Moreover, the frequency dispersion of the dielectric constant increases with temperature and this increase is more pronounced at lower frequencies ( $\epsilon=123$  at 40 °C and 540 at 140 °C for a measurement frequency of 1 kHz). The dielectric losses were found to have values ranging between 0.2 and 0.4 for all frequencies at 40 °C and 1 at 140 °C for the same operating frequency. The experimental data suggested that, in terms of the dielectric loss the assembly of the magnetic grains and dielectric shells does not improve significantly the electric properties of the nanocomposites.

Mornet and coworkers proposed an interesting soft-solution route for the preparation of functional ferroelectric-ferro/ferrimagnetic nanocomposites [70]. In the first step commercial perovskite (BaTiO<sub>3</sub> and/or Ba<sub>0.6</sub>Sr<sub>0.4</sub>TiO<sub>3</sub>) nanoparticles with different sizes (50-150 nm) were coated with a layer of SiO<sub>2</sub> and then their surface was modified by coupling aminosilane groups to induce positive charges (Figures 10a and b). This solution was treated with a ferrofluid containing superparamagnetic 7.5 nm  $\gamma$ -Fe<sub>2</sub>O<sub>3</sub> nanoparticles coated with a silica layer (shell thickness  $\approx$  2 nm) whose surfaces were negatively charged upon addition of citric acid (Figure 10c). These two solutions were subsequently mixed together and ferroelectric-superparamagnetic ceramic nanostructures were obtained by electrostatic



assembly between the aminated iron oxide nanograins and the perovskite nanoparticles (Figure 10e). The iron-oxide/perovskite particles can be assembled into 3D colloidal crystals via a sedimentation step (Figure 10d) followed by a drying and sintering process which yields a dense ferroelectric/superparamagnetic composite material and, at the same time, prevents interdiffusion and grain growth processes and preserves the individual building blocks distinct. The silica layer has proven to play a key role in the formation of ceramic nanocomposites because (i) it stabilizes the ferroelectric particles by playing a role of dielectric barrier between them, (ii) acts as a binding agent between the magnetic and dielectric phase and (iii) prevents the conductivity percolation among the iron oxide nanoparticles.

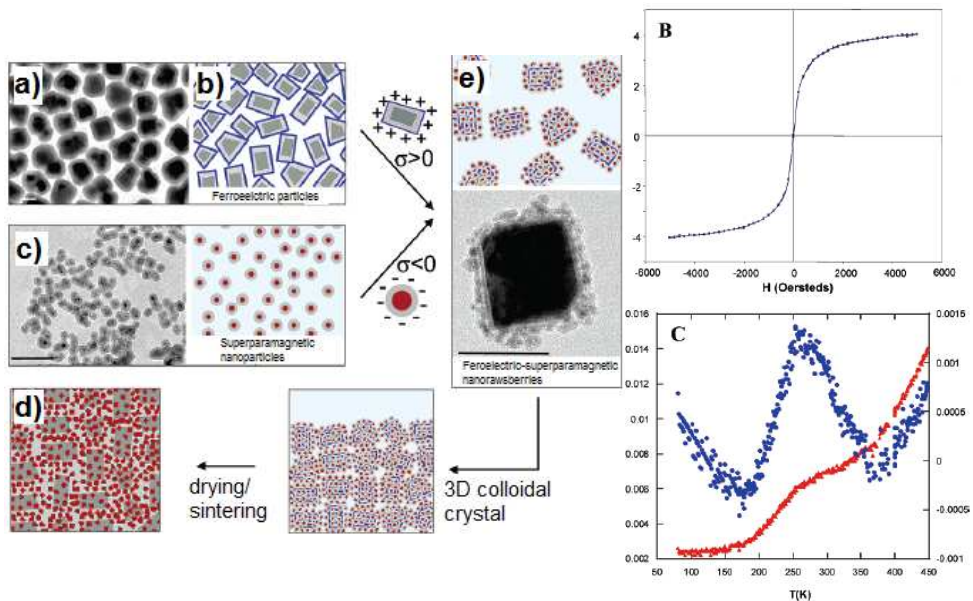


Fig. 10. Schematic of the successive steps used by Mornet and coworkers to fabricate perovskite-iron oxide core-shell ceramic nanocomposites, 3D colloidal crystals and dense powders

Interestingly, the  $\gamma$ - $\text{Fe}_2\text{O}_3$  did not convert to  $\alpha$ - $\text{Fe}_2\text{O}_3$  (non-magnetic), as seen in Fig. 10b, which suggests that the silica layer protects them during the thermal annealing and stabilize the constituent phases and prevents their coalescence and interdiffusion. It has been found that the dielectric permittivity can be controlled by adjusting the thickness of the silica layer, as well as the size of the perovskite particles. For example, in Fig. 10c is displayed the temperature variation of the imaginary part of the dielectric permittivity which shows a maximum at 270 K, which is the transition temperature of  $\text{Ba}_{0.6}\text{Sr}_{0.4}\text{TiO}_3$ . The electron microscopy micrographs of the nanopowders show that the morphology of the ceramic nanoparticles is preserved upon sintering at high temperature (Figure 11a), whereas the resonance amplitude decreases progressively and disappears at temperatures up to 430 K, which crosses the ferroelectric-paraelectric temperature of the perovskite phase ( $T_c=405$  K; Figure 11b).

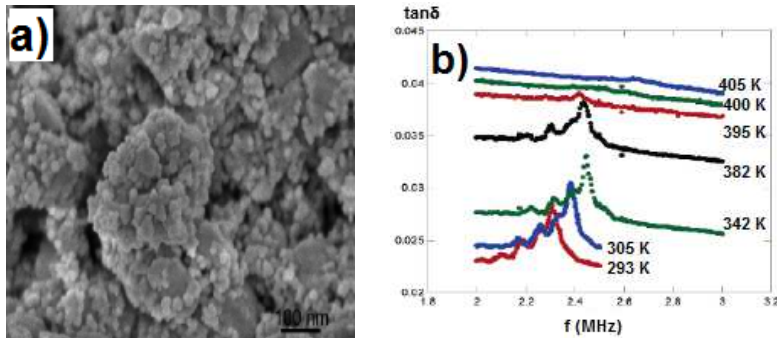


Fig. 11. (a) SEM image of the  $\gamma\text{-Fe}_2\text{O}_3\text{@SiO}_2/\text{BaTiO}_3\text{@SiO}_2$  nanocomposites; (b) the frequency dependence of the piezoelectric amplitude of the nanopowders at different temperatures

Although the synthetic methodologies described above lead to the formation of core-shell ferroelectric/magnetic nanoparticles, the modification of their surfaces in such a way that they are soluble in polar solvents and, therefore, can be used in biomedical application is difficult. We describe in the following two different alternate strategies which can enable the post-synthesis functionalization of the nanoparticles. Two-phase ME nanoparticulate composites with a core-shell structure can be fabricated by a sequential bottom-up approach which combines a hydrolytic route with the liquid phase deposition (LPD). In the first step aqueous-based ferrofluids containing nearly monodisperse, water-soluble ferrite nanoparticles with different sizes and chemical compositions will be prepared by the complexation and controlled hydrolysis of metal transition ions in diethyleneglycol solutions at 250 °C. The formation of the metal oxide nanoparticles takes place through three successive steps depicted in Fig. 10 and leads to highly stable colloidal solutions in polar solvents, due to the passivation of the individual nanocrystals with polyol molecules [71,72]. The size of the magnetic nanocrystals can be controlled by adjusting the complexing power of polyol solvent (Figure 12).

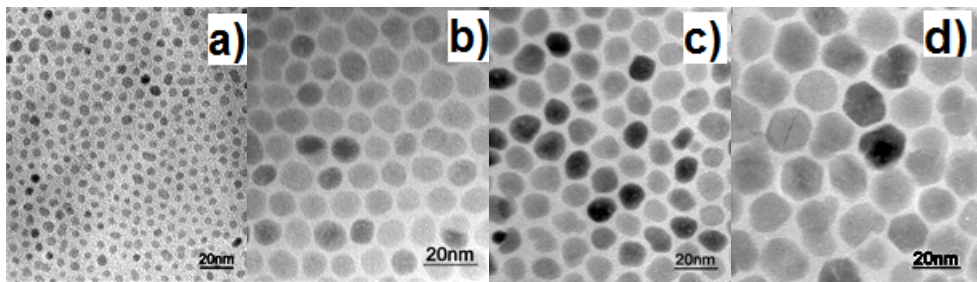


Fig. 12. (a) TEM images of monodisperse  $\text{Fe}_3\text{O}_4$  nanoparticles with a diameter of (a) 6 nm; (b) 10 nm; (c) 14 nm and (d) 18 nm obtained in polyol/polyamine solutions

In the next step a uniform piezoelectric shell can be deposited on each individual magnetic nanoparticle by mixing the ferrofluid with a treatment solution in which metal-fluoro complexes are slowly hydrolyzed at temperatures below 50 °C. This method, called the liquid phase deposition (LPD) consists of the progressive replacement of the fluoride ions in

the inner coordination sphere of the metal fluoro-complex by  $\text{OH}^-$  ions and/or water molecules with formation of the desired metal oxide. The hydrolysis rate can be controlled by temperature and/or by the consumption of the  $\text{F}^-$  ions by a fluoride scavenger such as  $\text{H}_3\text{BO}_3$  which forms water soluble complexes with the fluoride ions and prevents the contamination of the as-deposited hydroxides/oxyhydroxides by fluorine. We have successfully used this methodology for the deposition of both highly uniform transition metal ferrite and perovskite films and nanotubular structures with tunable chemical composition and controllable magnetic and ferroelectric properties [73]. As seen in Figure 13b the coating of the ferrite nanoparticles with the ferroelectric layer has a substantial effect on their magnetic properties: while the 14 nm  $\text{CoFe}_2\text{O}_4$  nanoparticles are superparamagnetic at room temperature,  $\text{CoFe}_2\text{O}_4@ \text{PbTiO}_3$  core-shell nanoparticles are ferrimagnetic and present a coercivity of about 1200 Oe. This is the result of the modification of the contributions of the surface anisotropy and dipolar interactions between the adjacent nanoparticles on the average magnetic moment of the nanocomposite [74,75]. A wide variety of spinel ferrite nanoparticles can be coated with perovskite layers, such as  $\text{BaTiO}_3$ ,  $\text{PbTiO}_3$  and  $\text{Pb}(\text{Ti}, \text{Zr})\text{O}_3$  and their properties can be controlled by adjusting both the size of the magnetic core and the thickness of the perovskite shell.

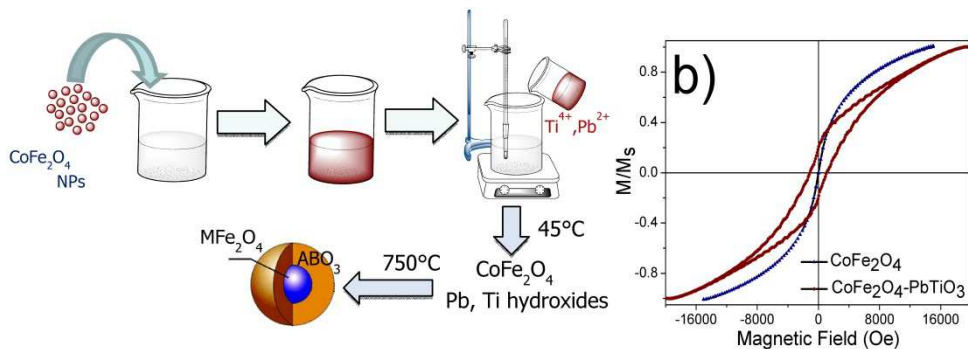


Fig. 13. (a) Schematic of the bottom-up synthetic strategy for the fabrication of ferrite-perovskite core-shell magnetolectric nanostructures by liquid phase deposition; (b) Room temperature hysteresis loops of the 14 nm  $\text{CoFe}_2\text{O}_4$  nanoparticles and  $\text{CoFe}_2\text{O}_4@ \text{PbTiO}_3$  core-shell nanoparticles

Moreover, upon treatment with a citric acid solution the ferroelectric-ferrimagnetic ceramic nanocomposites are passivated, thereby forming stable colloidal solutions in water and other polar solvents. Another synthetic methodology for the preparation of functional ferroelectric-ferro/ferrimagnetic nanocomposites consists of assembling pre-synthesized, monodisperse spinel and perovskite colloidal nanoparticles using stable oil-water microemulsion systems. Well-dispersed, size-uniform ferrite and perovskite nanoparticles can be mixed together in a stable micellar solution and confined in the oil microemulsion droplets [63]. The subsequent evaporation of the low-boiling solvent from the colloidal solution leads to a shrinkage of the individual droplets, decreasing of the distances between the nanoparticles which will stick together to form 3D spinel-perovskite colloidal spheres. This technique has been used for assembling either particles with the same chemical composition, such as  $\text{Ag}_2\text{Se}$ ,  $\text{BaCrO}_4$ ,  $\text{CdS}$ ,  $\text{Au}$ ,  $\text{Fe}_3\text{O}_4$  [76-79] or dissimilar nanoparticles,

such as  $\text{Fe}_3\text{O}_4$  and Au [80] and CdSe/CdS, respectively [78]. The resulting nanoparticles can be dispersed in aqueous solutions since the capping agents passivating each individual nanoparticle interdigitate with those from the neighboring nanocrystals via hydrophobic Van-der-Waals interactions. Another advantage of this method is that the amount of ferrite phase in the nanocomposite can be varied in a wide range will be used for the optimization of the ME coupling coefficient.

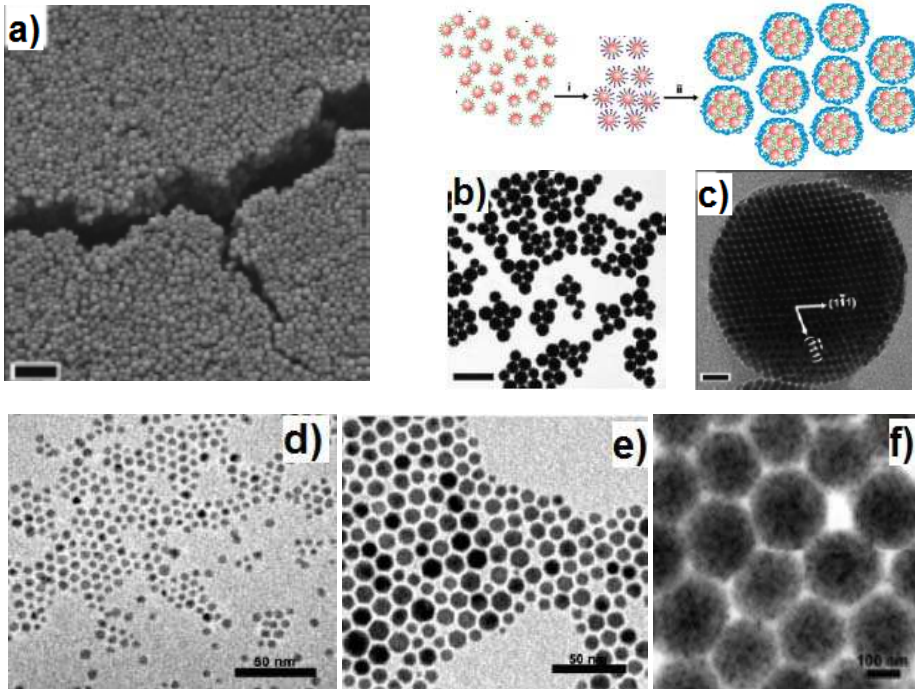


Fig. 14. (a) SEM image of multilayered assemblies of  $\text{Fe}_3\text{O}_4$  superparticles with an average diameter of 190 nm; (b) and (c) TEM images of the 190 nm superparticles. The scale bars are: 1  $\mu\text{m}$  (a); 500 nm (b) and 20 nm (c), respectively (Ref.63)

This method was used for the synthesis of colloidal superparticles, whereby the diameter of the colloidal spheres can be adjusted in a wide range, typically from 80 to 350 nm by controlling the size of the microemulsion droplets.

#### *Fabrication of spinel-perovskite core-shell nanotubular structures*

Another type of core-shell ferroelectric-ferromagnetic nanostructures with potential applications in the biomedical field is represented by coaxial nanotubular/nanorod structures. Xie and coworkers have recently reported on the fabrication of  $\text{CoFe}_2\text{O}_4$ - $\text{PbZr}_{0.52}\text{Ti}_{0.48}\text{O}_3$  core-shell nanofibers using a sol-gel process and coaxial electrospinning. [81] Two different solutions, containing the precursors for the ferrite and perovskite phases combined with polymethyl methacrylate (PMMA) and poly(vinyl) pyrrolidone (PVP) were electrospun by using a coaxial spinneret consisting of two commercial blunt needles with different lengths and diameters (Figures 15a and b). A voltage of 1.2 kV/cm was applied to

the needle and the resulting nanofibers were heated at 750 °C in air for 2 h to induce the crystallization of the oxide phases and eliminate the organic components.

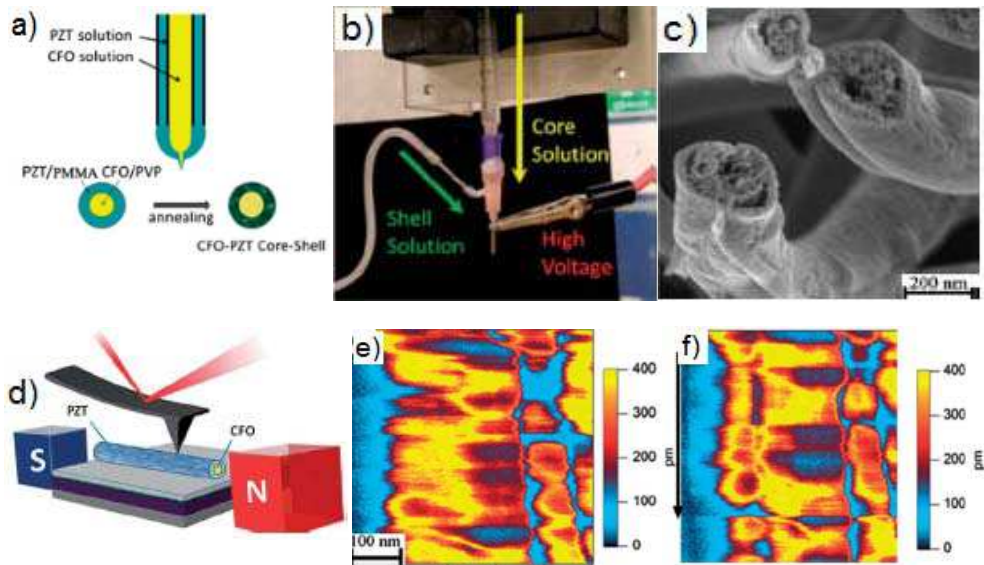


Fig. 15. (a) and (b) Schematic and a picture of the experimental setup used for the fabrication of core-shell nanofibers by electrospinning; (c) SEM image of a core-shell nanofibers; (d) Schematic of the PFM measurement of an individual ferrite-perovskite core-shell fiber; amplitude PFM contrast images of one composite fiber without (e) and in the presence of an external magnetic field (f)

The SEM image of one individual fiber (Fig. 15 c) shows that, indeed, a core-shell structure can be obtained by this approach; however, the magnetic core is porous compared to the perovskite shell, which looks much more compact. Such a discrepancy between the porosity of the core and shell components of the composite fiber can be detrimental for the ME coupling since the interfaces are not uniform and local chemical heterogeneities and gaps are present at the interphase boundaries. The existence of a local magnetoelectric coupling between the ferrite and perovskite phases was proven qualitatively by recording the amplitude PFM contrast images of one single fiber without and with a magnetic field. As seen in Figures 15e and f, the ferroelectric domain structure of the nanofibers is significantly altered when a magnetic field is applied, which suggests that an elastic coupling between the ferrite core and perovskite shell is induced by the magnetic field.

Nanotubular ferroelectric and magnetostrictive structures, as well as ME coaxial architectures can be fabricated by a template-assisted liquid phase deposition (LPD) method. This synthetic strategy is schematized in Figure 16. In the first step, ferroelectric nanotubes are deposited into the pores of alumina membranes (AAM) by the controlled hydrolysis of metal fluoro-complexes under mild conditions (Fig. 16a) similar to those used to create a perovskite shell around each individual water-soluble ferrite nanoparticle. The outside diameter of the tubes is determined by the size of the pores of the membrane and can be controlled in the range from 20 to 200 nm. In the second step the ferroelectric

nanotubes immobilized within the pores of the membranes will be filled with a spinel ferrite leading to the formation of coaxial magnetoelectric ceramic nanostructures (Figure 16b).

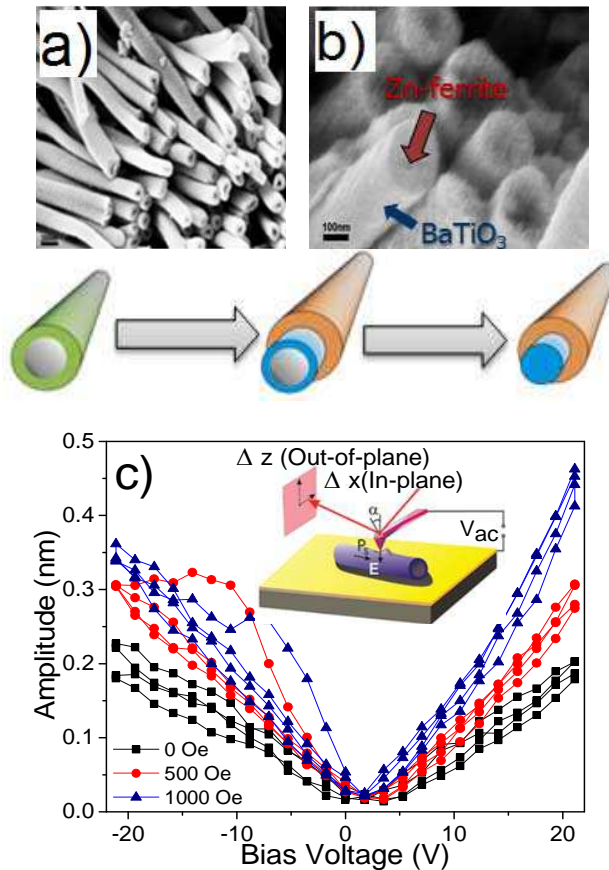


Fig. 16. (a) Side view FE-SEM image of  $\text{CoFe}_2\text{O}_4$  (CFO) nanotubes with a diameter of 200 nm; (b) Side view FE-SEM image of  $\text{BaTiO}_3$ - $\text{CoFe}_2\text{O}_4$  coaxial nanowires obtained by filling the perovskite nanotubes with  $\text{CoFe}_2\text{O}_4$ ; (c) Probing the ME response of an individual BTO-CFO coaxial nanowire by measuring its piezoelectric signal under different magnetic fields

Finally, the membranes are dissolved upon treatment in an alkaline solution, yielding free-standing spinel-perovskite coaxial 1-D nanostructures. Optimization of the ME properties of these structures will be carried out by either changing the chemical composition of the oxide nanotubes, or by varying the spinel/perovskite ratio which can be achieved by changing the wall thickness of the shell (a structural parameter which is hard to control in the sol-gel approaches conventionally used in the synthesis of oxide nanotubes). The magnetolectric coupling between the oxide phases in these 1-D nanocomposites was proven by piezoresponse force microscopy (PFM) in the presence of a magnetic field. As seen in Figure 16c, there is a notable change in the amplitude of the PFM signal and the slope of the experimental curves when a magnetic field is applied in the plane of the coaxial

nanostructure, indicating that the piezoelectric deformation of the nanocomposite is influenced by the magnetic field. The value of the ME coupling coefficient calculated from the slope of the butterfly-loops is  $\alpha_E=1.08$  V/cm Oe, which indicates a strong elastic coupling between the constituent phases of the nanocomposite.

### Future applications

One of the areas where control of channel gating may be of particular importance is generation of action potentials in neurons. When neurons are not being stimulated and not conducting impulses, their membrane is polarized. This so called resting potential is of the order of 70-90 mV for typical cells and it is a measure of an imbalance of sodium and potassium ions across the membrane resulting from the interplay between several mechanisms of ion transport coexisting in the membrane. The active mechanisms (such as sodium-potassium pumps) require energy from ATP phosphorylation to “pump” ions against the concentration gradient, while passive mechanisms (such as ion channels) flux the ions down their gradients. As a result, there is a higher concentration of sodium on the outside than the inside and a higher concentration of potassium on the inside than the outside. The resting potential will be maintained until the membrane is disturbed or stimulated. If the stimulus is sufficiently strong, an action potential will occur.

An action potential is a very rapid change in membrane potential that occurs when a nerve cell membrane is stimulated. During the time course of the action potential, the membrane potential goes from the resting value (typically -70 mV) to some positive value (typically about +30 mV) in a very short period of time, of the order of a few ms. Action potentials are triggered by stimuli that can alter the potential difference by opening some sodium channels in the membrane. The stimulus can be for instance the binding of neurotransmitters to ligand gated ion channels or the membrane can be directly stimulated electrically from a glass pipette through a patch clamp. Once the potential difference reaches a threshold voltage (typically 5 - 15 mV less negative than the resting potential), it starts a chain of events (opening and closing of potassium channels) that leads to the action potential. This phenomenon has been first described mathematically in the celebrated Hodgkin-Huxley model [82].

As we mentioned action potentials can be triggered chemically (neurotransmitter binding) or electrically, as a result of membrane depolarization caused by electric impulses delivered locally through an electrode or globally by electric shock. The drawback for the electrode stimulation is that it is highly invasive and therefore of a very limited applicability for therapy, while the electric shock is global and makes targeted stimulation very difficult. This is, however, the basis for neuroscience research as well as electrostimulation therapy, for instance for pain. Using multiferroic nanoparticles seems very promising alternative to these techniques. The method we describe can be used for membrane stimulation and it eliminates the main drawbacks of hitherto used methods: it is noninvasive and localized. It can be used for localized stimulation and triggering of action potentials in studies of neural connectivity, and it can potentially become an effective pain treatment.

Emerging research on multiferroic materials is primarily seeking applications in information technology and wireless communication [7,8]. This work seems to be first to indicate great potential of these new materials in biology and medicine. Stimulation of the nervous system by means of defibrillators, electroshock, or other electro-physical therapy devices for resuscitation, depression therapy, or pain treatment utilizes high voltages and affects large

portions of a patient's body. On the other hand, locally applicable electro-physical devices such as pace makers or contemporary acupuncture equipment require invasive methods to be implemented (surgery or puncture).

The method proposed in this article takes advantage of nanotechnology to stimulate functions on the cellular level by remotely controlling voltage generated by nanosized objects placed either inside or outside the cells in their close vicinity. Although this article targets ion channels to control the ion transport across membranes of mammalian cells, the multiferroic particles have potential for new applications in other fields of biology and medicine. For instance, the signals generated by nanoparticles have similar characteristics to those of the electric signals propagating in the neural cells. Therefore, it can be expected that the electric fields of the nanoparticles can interfere with the signals received by the neural cells. The magnitude and the shape of the signals generated by the nanoparticles can be controlled by the time characteristics of the external magnetic field. This creates an opportunity to remotely stimulate functions of neural cells for pain treatment or for enhancing response of damaged cells.

Another unexplored area of research is the effect of electric fields generated by the multiferroic nanoparticles inside the cell on the organelles and DNA. Electric field may have either stimulating or damaging effect on cells, depending on its strength and frequency. Strong static fields may result in electrolysis of the cytoplasm, electroporation etc., and high frequency electromagnetic fields can cause local hyperthermia. Current research and existing physical-therapy devices use global electric fields and the response of organelles to fields delivered locally is unknown. It is likely that strong enough electric fields inside cells can significantly perturb the functions of their organelles. This opens a possibility to use multiferroic nanoparticles for cancer treatment by a method different from chemotherapy or hyperthermia. Interestingly, the multiferroic particles may have a dual function depending on the frequency of the applied magnetic field. The magnetic component of the particles can be used at high frequencies (in the radio- or microwave range) for hyperthermia whereas it can generate electric signals for stimulation of membranes or organelles in the acoustic (kHz) frequency range. At this point it is important to notice that the values of magnetoelectric voltage coefficient (1V/cmOe) used in our estimates refer to non-resonant performance of the composite nanoparticles. This coefficient can be enhanced by a factor of 100 by applying magnetic field pulses with higher frequencies (in MHz or GHz) which correspond to electromechanical resonance. Although ion channels may not respond to these high frequency fields, the strength of the electric fields produced by the nanoparticles may be sufficient to cause irreversible electroporation of the cell membranes and consequently their damage. This effect can provide alternative tool for cancer treatment and be used separately (for short series of pulses) or jointly with hyperthermia (for longer series). Also, static magnetic field can be used to drag the particles to certain organs for highly targeted applications. More intriguing problem is to recognize the effects of weaker fields. There have been reports indicating some effect on cell proliferation and growth, ionic transport, and neural signaling [83-85]. The method we proposed opens unique opportunities in this area. Composite multiferroic particles are ideal objects to produce electric fields on submicrometer scale which have never been tested. We anticipate great potential for applications of multiferroic nanoparticles in several fields of biomedicine, such as cancer research, neurology, brain functions, pain treatment, and we strongly believe that the necessary technology exists and these applications will soon be put to test.



## 2. Acknowledgments

The authors acknowledge financial support through DARPA grant HR0011-09-1-0047.

## 3. References

- [1] W. Andrä, U. Häfeli, R. Hergt and R. Misri, "Applications of magnetic particles ion medicine and biology", in: Handbook of Magnetism and Advanced Magnetic Materials, ed. H. Kronmüller, S. Parkin Vol. 4 (Novel Materials) pp.2536-2568, John Wiley & Sons 2007
- [2] J.M.D. Coey, in: Magnetism and Magnetic Materials, Cambridge University Press, USA 2010, pp. 555-565
- [3] P. Moroz, S.K. Jones and B.N. Gray, Magnetically mediated hyperthermia, current status and future directions, *International Journal of Hyperthermia* 18 (2002) 267-284
- [4] H. Huang, S. Delikanli, H. Zeng, D.M. Ferkey and A. Pralle, "Remote control of ion channels and neurons through magnetic-field heating of nanoparticles", *Nature Nanotechnology* 5 (2010) 602-606
- [5] J. Dobson, "Nanomagnetic actuation: remote control of cells", *Nature Nanotechnology* 3 (2008) 139-143
- [6] L.W. Martin, S. P. Crane, Y-H. Chu, M. B. Holcomb, M. Gajek, M. Huijben, C-H. Yang, N. Balke and R. Ramesh Multiferroics and magnetoelectrics: thin films and nanostructures *J. Phys.: Condens. Matter* 20 (2008) 434220
- [7] C. W. Nan, M. I. Bichurin, S. Dong, D. Viehland and G. Srinivasan, "Multiferroic magnetoelectric composites: Historical perspective, status, and future direction", *J. Appl. Phys.* 103 (2008) 031101, pp.1-35
- [8] M. Fiebig, "Revival of the magnetoelectric effect", *J. Phys. D: Appl. Phys.* 38 (2005) R123-R152
- [9] W. Eerenstein, N. D. Mathur and J. F. Scott, "Multiferroic and magnetoelectric materials", *Nature* 442 (2006) 759-765
- [10] C. Foged, B. Brodin, S. Frokjaer and A. Sundblad, "Particle size and surface charge affect particle uptake by human dendritic cells in an in vitro model, *Int. J. Pharmaceutics* 298 (2005) 315-322
- [11] C. N. R. Rao and C. R. Serraoab," New routes to multiferroics", *J. Mater. Chem.* 17 (2007) 4931-4938
- [12] M. I. Bichurin, V. M. Petrov, S. V. Averkin, and E. Liverts, "Present status of theoretical modeling the magnetoelectric effect in magnetostrictive-piezoelectric nanostructures. Part I: Low frequency and electromechanical resonance ranges" *J. Appl. Phys.* 107 (2010) 053904 pp.1-11
- [13] M. I. Bichurin, V. M. Petrov, S. V. Averkin, and E. Liverts," Present status of theoretical modeling the magnetoelectric effect in magnetostrictive-piezoelectric nanostructures. Part II: Magnetic and magnetoacoustic resonance ranges" *J. Appl. Phys.* 107 (2010) 053905 pp.1-18
- [14] R. Liu, Y. Zhao, R. Huang, Y. Zhao, and H. Zhou, "Multiferroic ferrite/perovskite oxide core/shell nanostructures" , *J. Mater. Chem.* 20 (2010) 10665-10670
- [15] K. Raydongia, A. Nag, A. Sundaresan, and C. N. R. Rao, "Multiferroic and magnetoelectric properties of core-shell  $\text{CoFe}_2\text{O}_4$ @ $\text{BaTiO}_3$  nanocomposites", *Appl. Phys. Lett.* 97 (2010) 062904 pp. 1-3

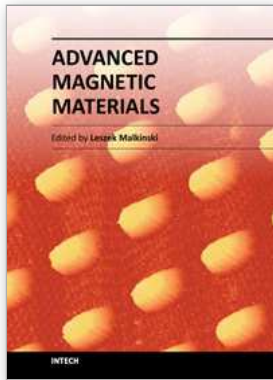
- [16] K. C. Verma, S. S. Bhatt, M. Ram, N. S. Negi, and R. K. Kotnala, "Multiferroic and relaxor properties of  $\text{Pb}_{0.75}\text{Sr}_{0.3}[\text{Fe}_{2/3}\text{Ce}_{1/3}(\text{O}_{0.12}\text{Ti}_{0.988})\text{O}_3$  and  $\text{Pb}_{0.75}\text{Sr}_{0.3}[\text{Fe}_{2/3}\text{La}_{1/3}(\text{O}_{0.12}\text{Ti}_{0.998})\text{O}_3$  nanoparticles", *Materials Chem. and Phys.* 124(2-3) (2010) 1188-1192
- [17] C.-C. Chang, L. Zhao, and M.-K. Wu, "Magnetolectric study in  $\text{SiO}_2$ -coated  $\text{Fe}_3\text{O}_4$  nanoparticle compacts", *J. Appl. Phys.* 108 (2010) 094105 pp. 1-5
- [18] R. P. Maiti, S. Basu, S. Bhattacharya, and D. Charkravorty, "Multiferroic behavior in silicate glass nanocomposite having a core-shell microstructure", *J. Non-Crystalline Sol.* 355(45-47) (2009) 2254-2259
- [19] V. Corral-Flores, D. Buano-Baques, R.F. Ziolo, Synthesis and characterization of novel  $\text{CoFe}_2\text{O}_4$ - $\text{BaTiO}_3$  multiferroic core shell nanostructures. *Acta Materialia* 58 (3) (2010) 764-769
- [20] M. Liu, H. Imrane, Y. Chen, T. Goodrich, Z. Cai, K. Ziemer, J. Y. Huang, and N. X. Sun, "Synthesis of ordered arrays of multiferroic  $\text{NiFe}_2\text{O}_4$ - $\text{Pb}(\text{Zr}_{0.52}\text{Ti}_{0.48})\text{O}_3$  core-shell nanowires", *Appl. Phys. Lett.* 90 (2007) 152501 pp. 1-3
- [21] V. M. Petrov, M. I. Bichurin, and G. Srinivasan, "Electromechanical resonance in ferrite-piezoelectric nanopillars, nanowires, nanobilayers, and magnetolectric interactions", *J. Appl. Phys.* 107 (2010) 073908, pp 1-6
- [22] P. Fulay, in: *Electronic, Magnetic and Optical Materials*, CRC Press, Taylor and Francis Group, LLC, USA, 2010
- [23] R.C. Smith, in: *Smart Material Systems: Model Development*, Society for Industrial and Applied Mathematics, USA 2005
- [24] B. Hille, *Ionic Channels of Excitable Membranes*. Sinauer Associates Inc., Sunderland Massachusetts 1992.
- [25] F.M. Ashcroft, *Ion Channels and disease*. Academic Press, San Diego, London 2000.
- [26] F. Bezanilla, E. Peroso, and E. Stefani. Gating of Shaker  $\text{K}^+$  channels: II. The components of gating currents and a model of channel activation. *Biophys. J.* 66 (1994) 1011-1021
- [27] W.N. Zagotta, T. Hoshi, and R.W. Aldrich. Potassium channel gating: III. Evaluation of kinetic models for activation. *J. Gen. Physiol.* 103 (1994) 312-362
- [28] M.M. Millonas and D.R. Chialvo. Control of voltage-dependent biomolecules via non-equilibrium kinetic focusing. *Phys. Rev. Lett.* 76 (1996) 550-553
- [29] H. Qian, From discrete protein kinetics to continuous Brownian dynamics: a new perspective. *Protein. Sci.* 11 (2002) 1-5
- [30] D. Sigg, H. Qian, and F. Bezanilla. Kramer's diffusion theory applied to gating kinetics of voltage-dependent ion channels. *Biophys. J.* 76 (1999) 782-803
- [31] D. Sigg and F. Bezanilla. A physical model of potassium channel activation: from energy landscape to model kinetics. *Biophys. J.* 84 (2003) 3703-3716
- [32] B. Sakmann and E. Neher. *Single-channel Recording*. Plenum Press, New York - London 1995.
- [33] Y. Jiang, et al. X-ray structure of a voltage-dependent  $\text{K}^+$  channel. *Nature* 423 (2003) 33-41
- [34] Y. Jiang, V. Ruta, J. Chen, A. Lee, and R. MacKinnon. The principle of gating charge movement in a voltage-dependent  $\text{K}^+$  channel. *Nature* 423 (2003) 42-48

- [35] A. Cha, G. E. Snyder, P. R. Selvin, and F. Bezanilla. Atomic scale movement of the voltage-sensing region in a potassium channel measured via spectroscopy. *Nature* 402 (1999) 809-813
- [36] M.C. Menconi, M. Pellegrini, M. Pellegrino, and D. Petracchi. Periodic forcing of single ion channel: dynamic aspects of the open-closed switching. *Eur. Biophys. J.* 27 (1998) 299
- [37] A. Kargol, A. Hosein-Sooklal, L. Constantin, and M. Przystalski. Application of oscillating potentials to the Shaker potassium channel. *Gen. Physiol. Biophys.* 23 (2004) 53-75
- [38] A. Kargol, B. Smith, and M.M. Millonas. Applications of nonequilibrium response spectroscopy to the study of channel gating. Experimental design and optimization. *J. Theor. Biol.* 218 (2002) 239-258
- [39] A. Kargol and K. Kabza. Test of nonequilibrium kinetic focusing of voltage-gated ion channels. *Phys. Biol.* 5 (2008) 026003
- [40] M.M. Millonas and D.A. Hanck. Nonequilibrium response spectroscopy of voltage-sensitive ion channel gating. *Biophys. J.* 74 (1998) 210229
- [41] C.R. Doering, W. Horsthemke, and J. Riordan. Nonequilibrium fluctuation-induced transport. *Phys. Rev. Lett.* 72 (1994) 2984
- [42] A. Fulinski, Noise-simulated active transport in biological cell membranes. *Phys. Lett. A* 193 (1994) 267
- [43] W. Horsthemke and R. Lefever. Noise-induced transitions in electrically excitable membranes. *Biophys. J.* 35 (1981) 415
- [44] K. Lee and W. Sung. Effects of nonequilibrium fluctuations on ionic transport through biomembranes. *Phys. Rev. E* 60 (1999) 4681
- [45] B. Liu, R.D. Astumian, and T.Y. Tsong. Activation of Na<sup>+</sup> and K<sup>+</sup> pumping modes of (Na,K)-ATPase by an oscillating electric field. *J. Biol. Chem.* 265 (1990) 7260
- [46] D.C. Camerino, T. Domenico, and J.-F. Desaphy. Ion channel pharmacology. *Neurotherapeutics* 4 (2007) 184-198
- [47] S.F. Cleary, "In vitro studies of the effects of nonthermal radiofrequency and microwave radiation", in: J.H. Bernhardt, R. Matthes, M. Repacholi (eds.) Non-thermal effects of RF electromagnetic fields. Proc. Intl. Seminar of the Biological effects of non-thermal pulse and amplitude modulated RF electromagnetic fields and related health hazards", Munich-Neuherberg, 20-22 Nov. 1996, 119-130
- [48] R.P. Liburdy "Biological interactions of cellular systems with time-varying magnetic fields", *Ann. N.Y. Acad. Sci.*, 649 (1992) 74-95
- [49] M.H. Repacholi, "Low-level exposure to radiofrequency electromagnetic fields: health effects and research needs", *Bioelectromagnetics* 19 (1998) 1-19
- [50] M.H. Repacholi, B. Greenebaum "Interaction of static and extremely low frequency electric and magnetic fields with living systems: health effects and research needs", *Bioelectromagnetics* 20 (1999) 133-160
- [51] A.D. Rosen "Effect of a 125 mT static magnetic field on the kinetics of voltage activated Na<sup>+</sup> channels in GH3 cells", *Bioelectromagnet.* 24 (2003) 517-523
- [52] J.E. Tattersall, I.R. Scott, S.J. Wood, J.J. Nettell, M.K. Bevir, Z. Wang, N.P. Somarisi, X. Chen, "Effects of low intensity radiofrequency electromagnetic fields on electrical activity in rat hippocampal slices", *Brain Res.* 904 (2001) 43-53

- [53] R.A. Deyo, N.E. Walsh, D.C. Martin, L.S. Schoenfeld, and S. Ramamurthy. A controlled trial of transcutaneous electrical nerve stimulation (TENS) and exercise for chronic low back pain. *N. Engl. J. Med.* 322 (1990) 1627-1634
- [54] J.S. Perlmutter and J.W. Mink. Deep brain stimulation. *Ann. Rev. Neurosci.* 29 (2006) 229-257
- [55] A.N. Morozovska, M.D. Glinchuk, and E.A. Eliseev, Phase transitions induced by confinement of ferroic nanoparticles. *Phys. Rev. B* 76 (2007) 014102
- [56] M.T. Buscaglia, V. Buscaglia, L. Curecheriu, P. Postolache, L. Mitoseriu, A.C. Ianculescu, B.S. Vasile, Z. Zhe, Z. and P. Nanni, Fe<sub>2</sub>O<sub>3</sub>@BaTiO<sub>3</sub> Core-Shell Particles as Reactive Precursors for the Preparation of Multifunctional Composites Containing Different Magnetic Phases. *Chem. Mater.* 22 (2010) 4740-4748, doi:10.1021/cm1011982
- [57] L.Q. Weng, Y.D. Fu, S.H. Song, J.N. Tang, J.Q. Li, Synthesis of lead zirconate titanate-cobalt ferrite magnetolectric particulate composites via an ethylenediaminetetraacetic acid-citrate gel process. *Scripta Mater.* 56 (2007) 465-468, doi:10.1016/j.scriptamat.2006.11.032
- [58] G. Srinivasan, E.T. Rasmussen, B.J. Levin, and R. Hayes, Magnetolectric effects in bilayers and multilayers of magnetostrictive and piezoelectric perovskite oxides. *Phys. Rev. B* 65 (2002) doi:13440210.1103/PhysRevB.65.134402
- [59] G. Srinivasan, E.T. Rasmussen, J. Gallegos, R. Srinivasan, Y.I. Bokhan, V.M. Laletin, Magnetolectric bilayer and multilayer structures of magnetostrictive and piezoelectric oxides. *Phys. Rev. B* 64 (2001) 214408, doi:214408
- [60] G. Srinivasan, C.P. DeVreugd, C.S. Flattery, V.M. Laetsin, and N. Paddubnaya, Magnetolectric interactions in hot-pressed nickel zinc ferrite and lead zirconate titanate composites. *Appl. Phys. Lett.* 85 (2004) 2550-2552, doi:10.1063/1.1795365
- [61] C.W. Nan, G. Liu, Y.H. Lin, Influence of interfacial bonding on giant magnetolectric response of multiferroic laminated composites of Tb<sub>1-x</sub>Dy<sub>x</sub>Fe<sub>2</sub> and PbZr<sub>x</sub>Ti<sub>1-x</sub>O<sub>3</sub>. *Appl. Phys. Lett.* 83 (2003) 4366-4368, doi:10.1063/1.1630157
- [62] R. Sun, B. Fang, L. Zhou, Q. Zhang, X. Zhao, H. Luo, Structure and magnetolectric property of low-temperature sintering (Ni<sub>0.8</sub>Zn<sub>0.1</sub>Cu<sub>0.1</sub>)Fe<sub>2</sub>O<sub>4</sub>/[0.58PNN-0.02PZN-0.05PNW-0.35PT] composites. *Curr. Appl. Phys.* 11 (2011) 37-42, doi:DOI: 10.1016/j.cap.2010.06.015
- [63] N. Zhang, W. Ke, T. Schneider, G. Srinivasan, Dependence of the magnetolectric coupling in NZFO-PZT laminate composites on ferrite compactness. *J. Phys. -Cond. Matter* 18 (2006) 11013-11019, doi:10.1088/0953-8984/18/48/029
- [64] L. Mitoseriu, V. Buscaglia, Intrinsic/extrinsic interplay contributions to the functional properties of ferroelectric-magnetic composites. *Phase Trans.* 79 (2006) 1095-1121, doi:10.1080/01411590601067284
- [65] R.Z. Liu, Y.Z. Zhao, R.X. Huang, Y.J. Zhao, H.P. Zhou, Multiferroic ferrite/perovskite oxide core/shell nanostructures. *J. Mater. Chem.* 20 (2010) 10665-10670, doi:10.1039/c0jm02602f
- [66] L.P. Curecheriu, M.T. Buscaglia, V. Buscaglia, L. Mitoseriu, P. Postolache, A. Ianculescu, P. Nanni, Functional properties of BaTiO<sub>3</sub>/Ni<sub>0.5</sub>Zn<sub>0.5</sub>Fe<sub>2</sub>O<sub>4</sub> magnetolectric ceramics prepared from powders with core-shell structure. *AIP Vol.* 107 (2010)

- [67] M.T. Buscaglia, C. Harnagea, M. Dapiaggi, V. Buscaglia, A. Pignolet, P. Nanni, Ferroelectric BaTiO<sub>3</sub> Nanowires by a Topochemical Solid-State Reaction. *Chem. Mater.* 21 (2009) 5058-5065, doi:10.1021/cm9015047
- [68] M.T. Buscaglia, V. Buscaglia, R. Alessio, Coating of BaCO<sub>3</sub> crystals with TiO<sub>2</sub>: Versatile approach to the synthesis of BaTiO<sub>3</sub> tetragonal nanoparticles. *Chem. Mater.* 19 (2007) 711-718, doi:10.1021/cm061823b
- [69] A. Lotnyk, S. Senz, D. Hesse, Formation of BaTiO<sub>3</sub> thin films from (110) TiO<sub>2</sub> rutile single crystals and BaCO<sub>3</sub> by solid state reactions. *Solid State Ionics* 177 (2006) 429-436, doi:10.1016/j.ssi.2005.12.027
- [70] S. Mornet, C. Elissalde, O. Bidault, F. Weill, E. Sellier, O. Nguyen, M. Maglione, Ferroelectric-based nanocomposites: Toward multifunctional materials. *Chem. Mater.* 19 (2007) 987-992, doi:10.1021/cm0616735
- [71] D. Caruntu, Y. Remond, N.H. Chou, M.J. Jun, G. Caruntu, J.B. He, G. Goloverda, C. O'Connor, V. Kolesnichenko, Reactivity of 3d transition metal cations in diethylene glycol solutions. Synthesis of transition metal ferrites with the structure of discrete nanoparticles complexed with long-chain carboxylate anions. *Inorg. Chem.* 41 (2002) 6137-6146
- [72] D. Caruntu, G. Caruntu, C.J. O'Connor, Magnetic properties of variable-sized Fe<sub>3</sub>O<sub>4</sub> nanoparticles synthesized from non-aqueous homogeneous solutions of polyols. *J. Phys. D-Appl. Phys.* 40 (2007) 5801-5809, doi:10.1088/0022-3727/40/19/001
- [73] A. Yourdkhani, A.K. Perez, C. Lin, G. Caruntu, Magnetolectric Perovskite-Spinel Bilayered Nanocomposites Synthesized by Liquid-Phase Deposition. *Chem. Mater.* 22 (2010) 6075-6084, doi:10.1021/cm1014866
- [74] C.R. Vestal, Z.J. Zhang, Synthesis and Magnetic Characterization of Mn and Co Spinel Ferrite-Silica Nanoparticles with Tunable Magnetic Core. *Nano Lett.* 3 (2003) 1739-1743, doi:10.1021/nl034816k
- [75] J.L. Dormann, D. Fiorani, E. Tronc, On the models for interparticle interactions in nanoparticle assemblies: comparison with experimental results. *J. Magn. Magn. Mater.* 202 (1999) 251-267, doi:10.1016/s0304-8853(98)00627-1
- [76] J.Q. Zhuang, H.M. Wu, Y.A. Yang, Y.C. Cao, Supercrystalline colloidal particles from artificial atoms. *J. Am. Chem. Soc.* 129 (2007) 14166, doi:10.1021/ja076494i
- [77] F. Bai, D.S. Wang, Z.Y. Huo, W. Chen, L.P. Liu, X. Liang, C. Chen, X. Wang, Q. Peng, Y.D. Li, A versatile bottom-up assembly approach to colloidal spheres from nanocrystals. *Angewandte Chemie-International Edition* 46 (2007) 6650-6653, doi:10.1002/anie.200701355
- [78] J.Q. Zhuang, A.D. Shaller, J. Lynch, H.M. Wu, O. Chen, A.D.Q. Li, Y.C. Cao, Cylindrical Superparticles from Semiconductor Nanorods. *J. Am. Chem. Soc.* 131 (2009) 6084, doi:10.1021/ja9015183
- [79] P.H. Qiu, C. Jensen, N. Charity, R. Towner, C.B. Mao, Oil Phase Evaporation-Induced Self-Assembly of Hydrophobic Nanoparticles into Spherical Clusters with Controlled Surface Chemistry in an Oil-in-Water Dispersion and Comparison of Behaviors of Individual and Clustered Iron Oxide Nanoparticles. *J. Am. Chem. Soc.* 132 (2010) 17724-17732, doi:10.1021/ja102138a
- [80] X. Zhang, J.S. Han, T.J. Yao, J. Wu, H. Zhang, X.D. Zhang, B. Yang, Binary superparticles from preformed Fe<sub>3</sub>O<sub>4</sub> and Au nanoparticles. *Cryst. Eng. Comm.* 13 (2011) 5674-5676, doi:10.1039/c1ce05664f

- [81] S. Xie, F. Ma, Y. Liu and J. Li, Multiferroic CoFe<sub>2</sub>O<sub>4</sub>-Pb(Zr<sub>0.52</sub>Ti<sub>0.48</sub>)O<sub>3</sub> core-shell nanofibers and their magnetoelectric coupling, *Nanoscale*, 3 (2011) 3152-3158
- [82] A. Hodgkin and A.F. Huxley. A quantitative description of membrane current and its application to conduction and excitation in nerve. *J. Physiol.* 116 (1952) 507-544
- [83] J. McCann, F. Dietrich, and C. Rafferty. The genotoxic potential and magnetic fields: an update. *Mutation Research* 411 (1998) 45-86
- [84] M.A. Macri, S. Di Luzio, and S. Di Luzio. Biological effects of electromagnetic fields. *Int. J. of Immunopathology and Pharmacology*, 15(2) (2002) 95-105
- [85] L. Huang, L. Dong, Y. Chen, H. Qi, and D. Xiao. Effects of sinusoidal magnetic field observed on cell proliferation, ion concentration, and osmolarity in two human cancer cell lines. *Electromagnetic Biology and Medicine*, 25(2) (2006) 113-126



## **Advanced Magnetic Materials**

Edited by Dr. Leszek Malkinski

ISBN 978-953-51-0637-1

Hard cover, 230 pages

**Publisher** InTech

**Published online** 24, May, 2012

**Published in print edition** May, 2012

This book reports on recent progress in emerging technologies, modern characterization methods, theory and applications of advanced magnetic materials. It covers broad spectrum of topics: technology and characterization of rapidly quenched nanowires for information technology; fabrication and properties of hexagonal ferrite films for microwave communication; surface reconstruction of magnetite for spintronics; synthesis of multiferroic composites for novel biomedical applications, optimization of electroplated inductors for microelectronic devices; theory of magnetism of Fe-Al alloys; and two advanced analytical approaches for modeling of magnetic materials using Everett integral and the inverse problem approach. This book is addressed to a diverse group of readers with general background in physics or materials science, but it can also benefit specialists in the field of magnetic materials.

### **How to reference**

In order to correctly reference this scholarly work, feel free to copy and paste the following:

Armin Kargol, Leszek Malkinski and Gabriel Caruntu (2012). Biomedical Applications of Multiferroic Nanoparticles, *Advanced Magnetic Materials*, Dr. Leszek Malkinski (Ed.), ISBN: 978-953-51-0637-1, InTech, Available from: <http://www.intechopen.com/books/advanced-magnetic-materials/biomedical-applications-of-multiferroic-nanocomposites>

# **INTECH**

open science | open minds

### **InTech Europe**

University Campus STeP Ri  
Slavka Krautzeka 83/A  
51000 Rijeka, Croatia  
Phone: +385 (51) 770 447  
Fax: +385 (51) 686 166  
[www.intechopen.com](http://www.intechopen.com)

### **InTech China**

Unit 405, Office Block, Hotel Equatorial Shanghai  
No.65, Yan An Road (West), Shanghai, 200040, China  
中国上海市延安西路65号上海国际贵都大饭店办公楼405单元  
Phone: +86-21-62489820  
Fax: +86-21-62489821

© 2012 The Author(s). Licensee IntechOpen. This is an open access article distributed under the terms of the [Creative Commons Attribution 3.0 License](#), which permits unrestricted use, distribution, and reproduction in any medium, provided the original work is properly cited.